Article

Endosome Targeting meso-Tetraphenylchlorin-Chitosan Nano-Conjugates for Photochemical Internalization

VIVEK SAMBHAJI GAWARE, Monika Hakerud, Asta Juzeniene, Anders Høgset, Kristian Berg, and Már Másson

Just Accepted

Endosome Targeting *meso*-Tetraphenylchlorin-Chitosan Nano-Conjugates for Photochemical Internalization

Vivek S. Gaware[1, 2], Monika Håkerud[2, 3], Asta Juzeniene[3], Anders Høgset[2], Kristian Berg[3], Már Másson[1*]

[1] Faculty of Pharmaceutical Sciences, School of Health Sciences, University of Iceland, Hofsvallagata 53, IS-107 Reykjavik, Iceland

[2] PCI Biotech AS, Strandveien 55, N-1366 Lysaker, Norway

[3] Oslo University Hospital, The Norwegian Radium Hospital, Institute for Cancer Research, Department of Radiation Biology, Montebello, N-0310 Oslo, Norway

ABSTRACT

Four amphiphilic covalently linked *meso*-tetraphenylchlorin-chitosan nano-conjugates were synthesized and evaluated for use in photochemical internalization (PCI) *in vitro* and *in vivo*. The synthetic protocol for the preparation of two different hydrophobic chlorin photosensitizers, 5-(4-aminophenyl)-10,15,20-triphenylchlorin and 5-(4-carboxyphenyl)-10,15,20-triphenylchlorin, was optimized. These mono-functional photosensitizers were covalently attached to carrier chitosan via silyl-protected 3,6-di-*O-tert*-butyldimethylsilyl-chitosan (Di-TBDMS-chitosan) with 0.10 degree of substitution per glucosamine (DS). Hydrophilic moieties such as trimethylamine and/or 1-methylpiperazine were incorporated with 0.9 DS to give fully water-soluble conjugates after removal of the TBDMS groups. A dynamic light scattering (DLS) study confirmed the formation of nanoparticles with a 140–200 nm diameter. These nano-conjugates could be activated at 650 nm (red region) light, with a fluorescence quantum yield (Φ_F) of 0.43–0.45, and are thus suitable

candidates for use in PCI. These nano-conjugates were taken up and localized in the endocytic vesicles of HCT116/LUC human colon carcinoma cells and upon illumination they substantially enhanced plasmid DNA transfection. The nano-conjugates were also evaluated in preliminary *in vivo* experiments in tumor-bearing mice showing that the nano-conjugates could induce a strong photodynamic therapy (PDT) and also PCI effects in treatment with bleomycin.

KEYWORDS: chitosan, nanoparticles, Di-TBDMS-chitosan, PCI, photosensitizer, Endosome, transfection.

INTRODUCTION

Photochemical Internalization (PCI) is a technology that utilizes amphiphilic photosensitizer (PS) molecules and light for a site-specific release of endocytosed macromolecules or chemotherapeutics into the cell cytosol, thereby addressing one of the significant challenges in macromolecular anticancer therapy.[1-4]

Like photodynamic therapy (PDT), the PCI technology has three possible mechanisms for tumor therapy: (i) direct cytotoxic effects on the tumor cells, (ii) vascular shutdown, and (iii) possible activation of the immune system. In addition, PCI also has a fourth and very important effect: site-specific photochemically-induced release of drugs from endocytic vesicles into the cytosol. Unlike in the case of PDT, in PCI the photosensitizers need to be located in the endocytic vesicles of the targeted cells for the release of endocytosed therapeutic agents by reactive oxygen species (ROS)-mediated rupture of the endocytic vesicles.

PCI can be used with biologically active molecules that have not been exploited in the clinic due to their inability to penetrate the plasma membrane to reach their intracellular targets. PCI has been demonstrated *in vitro* and *in vivo* with type I ribosome-inactivating proteins[5], immunotoxins[6], adenovirus[7], nucleic acids[8], (plasmids, siRNA, mRNA) and chemotherapeutic drugs like bleomycin[9, 10] and doxorubicin[11]. Therefore, in principle PCI can be used for the treatment of many types of cancers[1] as well as for non-malignant diseases.[2-4, 12, 13] The main clinical advantage of PCI is the possibility for site-specific drug delivery leading to better utilization of drugs, thereby potentially reducing some of the severe side effects seen with most current cancer therapies.[4, 14, 15]

With PCI, the structure of the PS employed is essential for the therapeutic outcome. Over the past decade, substantial efforts have been put into developing various classes of PSs for better light absorption, greater tumor specificity, and less cutaneous photosensitivity compared to the first-generation photosensitizer Photofrin for PDT. In most cases, second generation PSs are based on porphyrin and chlorin structures as they often accumulate preferentially in neoplastic lesions as compared to the surrounding normal tissue. Chlorins are preferred over porphyrins for PDT and PCI as they offer the use of light with a deeper tissue penetration. This is due to their increased absorption on the red end of the spectrum and because they often have a very good singlet oxygen quantum yield.[2, 16] For effective PCI, however, the PS must also localize in endocytic vesicles. Amphiphilic PSs have been found to be the most efficient for PCI as their hydrophilic part prevents them from passing through the plasma membrane, allowing accumulation of the PS in the inner leaflet of the endocytic vesicles.[8] Therefore, PSs like *meso*-tetraphenylporphyrin disulfonate (TPPS$_{2a}$) and aluminum phthalocyanine disulfonate (AlPcS$_{2a}$) are very effective in PCI. *Meso*-Tetraphenylchlorin disulfonate (TPCS$_{2a}$, fimaporfin) is a similar PS that like TPPS$_{2a}$ and AlPcS$_{2a}$ has sulfonate groups in adjacent positions; and that is currently

3

being tested in clinical trials. A clinical Phase I fimaporfin dose escalating study in patients with cutaneous or sub-cutaneous head and neck and skin neoplasms has recently been completed. In this study fimaporfin was used in combination with the cytotoxic drug bleomycin, and the results indicated a strong tumor response in most treated tumors, with good safety. [17] A Phase I/II safety and efficacy study of fimaporfin in combination with gemcitabine for bile duct (cholangiocarcinoma) cancer has recently been initiated.[18, 19]

In order to further optimize the efficacy and selectivity of PDT, different strategies have been conceived, in which PSs are covalently attached to targeting vehicles. Thus, monoclonal antibodies (Mabs),[20-22] other proteins,[23, 24] polymers[25-30] and sugars,[31-35] have been designed to improve cell type-specific targeting. With this approach, a wide range of selective targets on the molecular, cellular, and tissue levels could be exploited. However, the use of large proteins, such as antibodies, often has limitations due to difficulties both in escaping from blood vessels and in moving through the interstitial space of the tumors. Still, macromolecules are very well suited for PCI since they usually get endocytosed through receptor-mediated endocytosis, adsorptive endocytosis, or pinocytosis. Polymer-PS conjugates could be a very good targeting system for PS in PCI since such structures could take advantage of the leaky vasculature and poor lymphatic drainage in tumors by the so-called enhanced permeability and retention (EPR) effect.

Chitosan is a very good polymer candidate as a carrier for PS attachment due to its non-toxic, biocompatible and biodegradable nature, as well as the fact that it can form nanoparticles spontaneously in aqueous conditions. In an earlier study, conjugation of free base *meso*-tetraphenylporphyrin (TPP) to cationic chitosan carriers has shown promising *in vitro* results for PCI mediated photochemical transfection.[36] We have developed a quantitative, reproducible and efficient synthetic method for the preparation of amphiphilic TPP-chitosan nano-conjugates with the aid of organo-soluble *tert*-butyldimethylsilyl protected chitosan (Di-TBDMS-chitosan). Using

this method, highly lipophilic PS mono-amino functionalized TPP (log P $\geq$ 9) was covalently

linked in a controlled manner (with a degree of substitution per glucosamine monomer (DS) of

0.10 or 0.25), followed by the incorporation of a hydrophilic moiety such as trimethylamine or 1-

methylpiperazine onto the chitosan backbone with a higher DS to enhance aqueous solubility.

With these structures, nano-conjugates with a DS of 0.10 of the photosensitizer (TPP in this case)

showed better properties in PCI-mediated photochemical transfection than nano-conjugates with

a DS of 0.25. While these porphyrin based TPP-chitosan nano-conjugates have shown promising

results *in vitro*, they are not optimal for use *in vivo*. This is mainly because porphyrin-based

molecules do not absorb enough light in the red region of the visible spectrum and thus would not

be activated in the deeper layers of the tumors.

Having established proof-of-concept with TPP, the logical next step was to synthesize

structurally similar chitosan nano-conjugates with a PS that would have a better absorbance in the

red spectral region. This could be achieved by converting porphyrin into chlorin by reducing one

of the pyrrolic double bonds of the tetrapyrrolic macrocycle. The synthesis of pure chlorin

derivatives is however considerably more challenging compared to that of porphyrins. In the

current study, we established a method for the synthesis of four different free base *meso*-

tetraphenylchlorin (TPC)-based TPC-chitosan nano-conjugates (with a DS of 0.10). To address

the challenge of synthesizing TPC conjugate two synthesis strategies were tried, starting from

either the carboxyl (-COOH) or the amino (-NH$_2$) derivative of the PS. In the former case the

"spacer" group, linking the PS to the biopolymer, will be slightly shorter and more rigid. Both

strategies were successful and the effect of the spacer group could therefore also be investigated.

These amphiphilic nano-conjugates are completely soluble in water and have been thoroughly

characterized by ^{1}H NMR, FT-IR, UV-vis spectrophotometry, fluorometry, and dynamic light

5

scattering (DLS). The molecular weight was determined by gel permeation chromatography (GPC) techniques. The efficacy of the TPC-chitosan nano-conjugates for PCI mediated gene delivery was evaluated *in vitro* using the HCT116/LUC human colon carcinoma cell line and *in vivo* using a xenograft model in nude mice.

EXPERIMENTAL SECTION

Materials

The chitosan (CS) polymer GO30626-2 (provided by Genis EHF, Iceland) was first converted to chitosan mesylate [weight-average molecular weight (Mw) = 10.5 kDa] and polydispersity index (PDI) = 1.04; degree of deacetylation (DD) = 95% (as determined by ^{1}H NMR)] by a previously reported procedure.[37] This was used as a starting material for the synthesis. Porphyrin and chlorin intermediate compounds were purified by flash column chromatography using silica gel 60 Å (0.040-0.063 mm) (230–400 mesh ASTM) which was purchased from Merck Millipore, Germany. The R_f values of compounds were determined by using thin layer chromatography (TLC) silica gel 60 F_{254} aluminum sheets, and compounds were visualized by ultraviolet (UV) and visible light. *M*eso-Tetraphenylporphyrin was purchased from Sigma-Aldrich, Germany and used as a reference compound for fluorescence quantum yield measurements. All other reagents and solvents were purchased commercially and used without further purification.

Equipment

Nuclear Magnetic Resonance (NMR) spectra were recorded on a DRX 400 MHz Bruker NMR spectrometer at 298 K and the chemical shifts were reported in parts per million (ppm) relative to

6

the residual proton signal (for ^{1}H NMR) and the carbon signal for (^{13}C NMR) of the deuterated

solvent used [^{1}H NMR: CDCl$_3$ (7.26 ppm), DMSO-d_6 (2.50 ppm); ^{13}C NMR: CDCl$_3$ (77.16

ppm), DMSO-d_6 (39.52 ppm)]. All coupling constants were reported in Hertz. The acetone peak

(2.22 ppm) was used as the internal reference for D$_2$O as solvents. The protons (*ortho*, *meta*,

para) on the phenyl rings of the porphyrin/chlorin system are identified with respect to their

positions relative to the porphyrins/chlorins ring system and not with the respective substituent

on the phenyl ring. Mass spectra were recorded on Bruker Autoflex III or a Bruker micro TOF-

Q11. The molecular mass of organic compounds was determined by high-resolution mass spectra

(HRMS) recorded on a Bruker micrOTOF-Q instrument with ESI. Fourier transform infrared

(FT-IR) spectra were recorded on an AVATAR 370 FT-IR instrument (Thermo Nicolet

Corporation, Madison, U.S.) by preparing sample pellets with KBr using a Specac compressor

(Specac Inc., Smyrna, U.S.). Melting Points (mp) were recorded on Buchi Melting Point B-540.

Polymer samples were dialyzed using Spectra/Por Dialysis Membrane (MWCO: 3500) and were

freeze dried on a Snijders Scientific freeze dryer. Water from MilliQ$^{®}$ (Millipore, Billerica, MA,

U.S.) with a resistivity above 18.2 MΩ·cm was used for all aqueous mobile phase and sample

preparation. PerkinElmer Lambda 35 UV-vis Spectrophotometer and LS 55 Fluorescence

Spectrometer were used for acquiring absorption and fluorescence emission spectra, respectively.

High performance liquid chromatography (HPLC) measurements were performed on Dionex

Softron GmbH (Germany) Ultimate 3000 series system. Gel permeation chromatography (GPC)

measurements were carried out on Dionex Softron GmbH (Germany) Ultimate 3000 series

system equipped with PSS´s ETA-2010 viscometer/Shodex RI-101 detectors. Dynamic Light

Scattering (DLS) and zeta potential measurements were performed on a Nanotrac wave-Zeta

(ZS), (Microtrac, U.S.) instrument having a scattering angle = 180°, a laser wavelength = 780 nm

and a power of 3 mW.

7

1
2
3
4
5
6
7
8
9
10
11
12
13
14
15
16
17
18
19
20
21
22
23
24
25
26
27
28
29
30
31
32
33
34
35
36
37
38
39
40
41
42
43
44
45
46
47
48
49
50
51
52
53
54
55
56
57
58
59
60

8

Methods

HPLC of Intermediate Porphyrin, and Chlorin Compounds

The purity (>95%) of porphyrin and chlorin intermediates was confirmed by HPLC, and for the

final TPC-chitosan nano-conjugates with GPC analysis and ^{1}H NMR analysis. HPLC

measurements were performed on a Dionex Softron GmbH (Germany) Ultimate 3000 series

consisting of a DGP-3600A pump with a built-in degasser, a WPS-3000 auto sampler, a TCC-

3100 column compartment and a Photodiode Array Detector (PDA-3000). A reverse phase

Phenomenex LUNA 5 μm C18 (2) column with size 150 × 4.60 mm (Phenomenex, UK), was

used for this purpose. All samples were prepared by first dissolving ~1 mg of compound in 100

μL DMSO, and then diluting it with CH_3CN in more than 10 fold this volume. Solutions were

filtered through a 0.45 μm (Spartan 13/0.45 RC, Whatman) filter before measurements. The flow

rate was 1.0 mL/min, the injection volume 20 μL and the temperature of the column

compartment was 25 °C. Four different wavelengths (254 nm, 366 nm, 420 nm and 650 nm) were

used for detection and recording. The isocratic mode was used for all measurements and the

mobile phase consisted of a three solvent system out of solvent A = 0.2% (v/v) TFA in CH_3CN,

solvent B = water, and solvent C = 10% (v/v) MeOH in water. In the mobile phase, retention time

and ratio of isomers (in case of chlorin derivatives) for individual compounds are shown in Table

S2, in the section *HPLC Results*.

Gel Permeation Chromatography of Chitosan Derivatives

Gel permeation chromatography (GPC) measurements of chitosan derivatives were performed

using WinGPC Unichrom software [Polymer Standards Service (PSS) GmbH (Germany)], on

Dionex HPLC system (auto sampler WPS-3000, Pump LPG-3400 A, Column compartment

9

TCC-3000), equipped with a series of three columns [Novema 10μ guard (50 × 8 mm), Novema 10μ 30A (150 × 8 mm) and Novema 10μ 1000A (300 × 8 mm)] and PSS´s ETA-2010 viscometer/Shodex RI-101 detectors. For GPC measurement of the parent chitosan material: eluent 0.1% (v/v) TFA in 0.1 M (aqueous) NaCl, and Poly(2-vinylpyridine) standards with varying average molecular weights (provided by PSS-kit), were used for generating a universal calibration curve. For GPC measurements of the chitosan mesylate and the final TPC-chitosan nano-conjugates (**18**, **19**, **23**, **24**): the eluent was 0.1 M (aqueous) NaCl, and Dextran standards with varyingaverage molecular weights (Amersham Bioscience AB, Sweden) were used for obtaining a universal calibration curve. All samples were dissolved in respective eluents and filtered through a 0.45 μm filter (Spartan 13/0.45 RC, Whatman) prior to measurements. GPC results consisting of viscosity and refractive index chromatograms were acquired at ambient temperature using the flow rate of 1 mL/min and with a 100μL sample volume.

Absorption and Fluorescence Properties

Absorption spectra were recorded on a PerkinElmer Lambda 35 UV-vis Spectrophotometer. Steady state fluorescence emission spectra were acquired on a PerkinElmer LS55 Fluorescence Spectrometer equipped with a red sensitive photomultiplier tube (R-928 PMT). The excitation source was a Xenon discharge lamp, equivalent to 20 kW for 8 μs duration and a Monk-Gillieson type monochromator was employed. For fluorescence quantum yield (Φ_F) measurements the conditions were as follows: (i) for small porphyrin and chlorin intermediate compounds, stock solutions were prepared in DMSO (0.01 mg/mL); the stock solution of the standard *meso*-tetraphenylporphyrin (TPP) (0.1 mg/mL) was prepared in toluene. (ii) For the final TPC-chitosan nano-conjugates (**18, 19, 23** and **24**) the following solutions were created: (a) for Φ_F measurements in DMSO, samples were dissolved by first add ing 100 μL of water to 1 mg of the

10

sample, it was then vortexed and finally 900 µL of DMSO was added and this solution was then further diluted ten times with DMSO and used as a stock solution; (b) for Φ_F measurements in H_2O, stock solutions were prepared by dissolving samples (0.1 mg/mL) in deionized H_2O. All the samples were wrapped in aluminum foil prior to analysis and used within 3 h of initial preparation.

The UV-vis absorption and fluorescence emission spectra were recorded at ambient temperature using a quartz cuvette with a 10 mm path length. For this purpose, diluted solutions with a final concentration below 10^{-6} M resulting in an absorbance of <0.1 for porphyrin derivatives and <0.04 for chlorin derivatives at the excitation wavelength were used to avoid an inner-filter effect. Fluorescence emission spectra of all the samples and reference compounds were measured under identical instrumental parameters: with the a constant slit width of 2.5 nm for both excitation and emission, auto PMT voltage, and spectra were averaged over three scans automatically by the acquisition software (FL WinLab software V4.00.03). For Φ_F calculations, fluorescence emission spectra were corrected for spectral sensitivity of the instrument (LS55 spectrometer) for PMT R-928, by calibration using a standard tungsten lamp (LS-1-CAL, LSC172 36251, Ocean optics, Dunedin, U.S.). The Φ_F values of all compounds (either in DMSO or H_2O) were determined relative to a standard TPP ($\Phi_F = 0.11$, in toluene $\lambda_{ex} = 514$ nm),[38] taking into account the refractive index of the solvents, using the following eq (1):[39]

$$(\Phi_F)_X = \Phi_{ST}\left(\frac{Grad_X}{Grad_{ST}}\right)\left(\frac{\eta_X^2}{\eta_{ST}^2}\right) \qquad (1)$$

Where, Φ_F = fluorescence quantum yield; Grad = gradient from the plot of integrated fluorescence intensity versus absorbance; η = the refractive index of the solvent; and the subscripts ST and X refer to the standard and the unknown test sample, respectively.

11

Dynamic Light Scattering (DLS)

For DLS and zeta potential measurements, TPC-chitosan (**18, 19** and **23, 24**) samples were dissolved in deionized water, sonicated (40 min, 55 °C), and then filtered through a 0.45 μm filter (Spartan 13/0.45 RC, Whatman) prior to measurements. All acquisitions were carried out at 25 ± 0.5 °C, and the results were the average of five runs of 30 s each, for each sample. The reproducibility within the same sample was checked by performing measurements at two different times and concentrations (0.1 mg/mL, and 1 mg/mL). The surface charge of the nano-conjugates was determined by the estimation of zeta potential.

Degree of Substitution (DS)

The DS of chlorin PSs in nano-conjugates (**18**, **19**, **23** and **24**) is determined by ^{1}H NMR of the key intermediate compounds **15** and **20**, by using the following eq (2):

$$DS = \left[\frac{\int (\text{Aromatic TPC peaks} + \alpha \text{ pyrrole NH peak})}{28} \right] \cdot \left[\frac{30}{\int (\text{TBDMS peaks})} \right] \qquad (2)$$

Where DS = degree of substitution of the photosensitizer per glucosamine monomer unit; Aromatic TPC peaks = sum of the integration of peaks of linked photosensitizer TPC$_{NIP}$ or TPC$_{CIP}$ moieties in the aromatic region; α pyrrole NH peak = sum of the integration of inner NH proton peaks of linked TPC$_{NIP}$/TPC$_{CIP}$ moieties in the aliphatic region; TBDMS peak = sum of the integration of peaks of TBDMS groups of backbone chitosan polymer in the aliphatic region.

Chemical Synthesis

meso-Tetraphenylporphyrin (1) (TPP). Porphyrin **1** was prepared by the procedure as described in our previous article following the literature procedure.[36, 40] TLC (Hexane/CH$_2$Cl$_2$, 1:1): R$_f$ = 0.66. FT-IR (KBr): ν = 3309 (N–H), 3051, 3022 (aryl C–H), 1595, 1556 (phenyl ring), 1469, 1440, 1347, 1176, 1001, 966, 793, 750, 726, 696, 657 cm^{-1}. ^{1}H NMR (CDCl$_3$): δ = 8.90 (s, 8H,

β-pyrrole-C*H*), 8.27 (d, *J = 8 Hz*, 8H, tetraphenyl-*Ho*), 7.75–7.83 (m, 12H, tetraphenyl-*Hm,p*), −2.70 (s, 2H, α-pyrrole-N*H*). ^{13}C NMR (CDCl$_3$): δ = 142.34 (q, *ipso-C*), 134.72 (t, *ortho-C*), 131.24 (br, β-pyrrole-*C*), 127.86 (t, *para-C*), 126.83 (t, *meta-C*), 120.31 (q, *meso-C*). HRMS (ESI): *m/z* calcd for C$_{44}$H$_{31}$N$_4$ ([M+H]$^+$), 615.2543; found, 615.2545.

5-(4-Aminophenyl)-10,15,20-triphenylporphyrin (**2**) *(TPP$_{N1}$)*. Amino-porphyrin **2** was prepared by the procedure as described in our previous article following the literature procedure.[36] TLC (Hexane/CH$_2$Cl$_2$, 3:7): R$_f$ = 0.23. FT-IR (KBr): *v* = 3470, 3381 (NH$_2$), 3314 (N–H), 3051, 3023 (aryl C–H), 1618, 1594, 1557 (aryl C–C), 1472, 1441, 1349, 1178, 1154, 1071, 1001, 965, 798, 746, 723, 699 cm^{-1}. ^{1}H NMR (CDCl$_3$): δ = 9.01 (d, *J = 4.0 Hz*, 2H, β-pyrrole-C*H*), 8.92–8.93 (m, 6H, β-pyrrole-C*H*), 8.29–8.31 (d, *J = 8 Hz*, 6H, triphenyl-*Ho*), 8.03 (d, *J = 8.0 Hz*, 2H, NH$_2$-phenyl-*Ho*), 7.77–7.84 (m, 9H, triphenyl-*Hm,p*), 6.99 (d, *J = 8.0 Hz*, 2H, NH$_2$-phenyl-*Hm*), 3.87 (s, 2H, N*H$_2$*), −2.62 (br s, 2H, α-pyrrole-N*H*) ppm. ^{13}C NMR (CDCl$_3$): δ = 146.12, 142.44, 142.39, 135.81, 134.71, 132.45, 131.21, 127.80, 126.81, 121.06, 120.15, 119.92, 113.52 ppm. HRMS (ESI): *m/z* calcd for C$_{44}$H$_{32}$N$_5$ ([M+H]$^+$), 630.2652; found 630.2660.

5-(4-Aminophenyl)-10,15,20-triphenylchlorin (**3**) *(TPC$_{N1}$)*. Amino-porphyrin **2** (1.5 g, 2.38 mmol) was dissolved in pyridine under N$_2$ while protected from light. To this solution, K$_2$CO$_3$ (2.96 g, 21.5 mmol) and *p*-toluenesulfonyl hydrazide (0.887 g, 4.77 mmol) were added and the resulting reaction mixture was heated under reflux. Additional portions of *p*-toluenesulfonyl hydrazide (0.887 g, 4.77 mmol) were added after the interval of 2, 4, 6 and 8 h. The stirring was continued under reflux for 24 h. The reaction mixture was then poured into EtOAc/H$_2$O (2:1, 900 mL) and heated under reflux for 1 h. After cooling to a 25 °C, the organic phase was separated and washed with 2 N HCl (3 × 200 mL) followed by a washing with H$_2$O (2 × 100 mL) and saturated aqueous NaHCO$_3$ (2 × 150 mL). The organic phase was then dried over Na$_2$SO$_4$ and

13

concentrated *in vacuo* to afford a 1.3 g crude product. Analysis of the visible spectrum of the crude product showed that it was a mixture of chlorin and bacteriochlorin (band at 651 and 737 nm, respectively). Furthermore, the analysis by ^{1}H NMR spectra confirmed that there was no trace amount of starting porphyrin material left unreacted.

This crude product (1.3 g) (chlorin and bacteriochlorin mixture) was dissolved in CH_2Cl_2 (100 mL) and then tetrachloro-*o*-benzoquinone (*o*-chloranil) (420 mg, 2.7 mmol) was added in one portion while stirring at 25 °C. The progress of the reaction was monitored simultaneously by UV-vis spectroscopy. As soon as the peak of bacteriochlorin (738 nm) had completely disappeared, the reaction mixture was quenched with solid sodium bisulfite ($NaHSO_3$) and washed with a 5% aqueous $NaHSO_3$ solution (2 × 125 mL), followed by a washing with H_2O (100 mL), 5% aqueous NaOH (2 × 150 mL), and finally with H_2O (150 mL). The organic phase was collected, dried over Na_2SO_4, and concentrated *in vacuo* to afford exclusively a chlorin compound, i.e. amino-chlorin **3** (1.2 g, 80%) as a brown colored solid. *Compound **3** and its derivatives exist in two isomeric forms (confirmed by HPLC).* TLC (Hexane/CH_2Cl_2, 3:7): R_f = 0.23. ^{1}H NMR (CDCl$_3$): δ = 7.86–8.66 (m, 14H, *β*-pyrrole-C*H* & tetraphenyl-*Ho*), 7.63–7.73 (m, 9H, triphenyl-*Hm,p*), 7.00 (d, *J = 8 Hz*, 2H, NH$_2$-phenyl-*Hm*), 4.14–4.23 (m, 4H, *chlorin β-pyrrole-CH$_2$*), 3.95 (br s, 2H, N*H$_2$*), −1.38 and −1.46 (br s, 2H, α-pyrrole-N*H*) ppm. HRMS (ESI): *m/z* calcd for C$_{44}$H$_{34}$N$_5$ ([M+H]$^+$), 632.2809; found 632.2808.

*5-(4-(2-(1-piperazinyl)acetyl)aminophenyl)-10,15,20-triphenylchlorin (**4**) (TPC$_{NIP}$).* Compound **3** (600 mg, 0.95 mmol) was dissolved in CH_2Cl_2 (15 mL) and stirred under N_2 while protected from light. To this solution, Et$_3$N (0.32 mL, 2.27 mmol) was added followed by a dropwise addition of chloroacetyl chloride (0.092 mL, 1.15 mmol) at 25 °C for 2 h. An excess quantity of piperazine (0.328 g, 3.8 mmol) was then added and the stirring was continued overnight. The reaction

14

mixture was diluted with CH_2Cl_2 (85 mL), washed with H_2O (3 × 35 mL) and brine (35 mL),

dried over Na_2SO_4, and concentrated *in vacuo*. The crude product was purified by silica gel

column chromatography using $MeOH/CH_2Cl_2$ (8:92) as eluent, to afford the desired compound **4**

(440 mg, 61%) as a brown solid. TLC (CH_2Cl_2/MeOH, 9:1): R_f = 0.15. ^{1}H NMR ($CDCl_3$): δ =

9.34, 9.39 (s, 1H, TPC-N*H*), 7.86–8.65 (m, 16H, *β*-pyrrole-C*H*, triphenyl-*Ho* & R-NHTPC-

phenyl-*Ho,m*), 7.66–7.73 (m, 9H, triphenyl-*Hm,p*), 4.18–4.19 (br s, 4H, *chlorin β*-pyrrole-C*H₂*),

3.29 (s, 2H, ArNHCOC*H₂*-pip), 3.17 (br m, 4H, piperazine ring-C*H₂*), 2.81 (br m, 4H, piperazine

ring-C*H₂*), −1.37 (br s, 2H, α-pyrrole-N*H*) ppm. ^{13}C NMR ($CDCl_3$): δ = 168.37, 167.48, 152.61,

143.14, 142.22, 140.86, 139.20, 138.32, 137.19, 136.99, 135.33, 134.64, 133.98, 133.01, 132.37,

132.12, 131.96, 128.17, 127.69, 126.81, 123.56, 123.38, 122.79, 122.08, 119.22, 117.94, 112.41,

111.65, 62.63, 53.50, 45.59, 35.90 ppm. HRMS (ESI): *m/z* calcd for $C_{50}H_{44}N_7O$ ($[M+H]^+$),

758.3602; found 758.3613.

Methyl-4-formylbenzoate (5). 4-Carboxybenzaldehyde (4 g, 26.6 mmol) was suspended in

anhydrous MeOH (60 mL) and stirred under N_2. The reaction mixture was cooled to 0 °C and

then acetyl chloride (9.5 mL, 133 mmol) was added dropwise. The resulting mixture was allowed

to warm up and then stirred for 12 h at 25 °C before it was concentrated *in vacuo* to remove the

MeOH completely. The crude residue was then diluted with EtOAc (120 mL), washed with 1 N

aqueous NaOH (5 × 30 mL) and brine (2 × 25 mL), dried over Na_2SO_4, and concentrated *in*

vacuo. The crude solid obtained was finally recrystallized with EtOAc and petroleum ether, to

afford the pure ester compound **5** (3.8 g, 87%) as a white solid. TLC (Hexane/CH_2Cl_2, 3:7): R_f =

0.36. mp: 61–63 °C (lit. mp 59–64 °C). ^{1}H NMR ($CDCl_3$): δ = 10.06 (s, 1H, C*H*O), 8.15 (d, *J = 8*

Hz, 2H), 7.91 (d, *J = 8 Hz*, 2H), 3.92 (s, 3H) ppm. ^{13}C NMR ($CDCl_3$): δ = 191.66, 166.07,

139.21, 135.13, 130.23, 129.55, 52.62 ppm.

5-(4-Methoxycarbonylphenyl)-10,15,20-triphenylporphyrin **(6)** *(TPP$_{MCl}$)*. Methyl-4-formylbenzoate **5** (2 g, 12.2 mmol) and benzaldehyde (3.7 mL, 36.6 mmol) was dissolved in CHCl$_3$ (800 mL) and stirred under N$_2$. To the reaction mixture, pyrrole (3.39 mL, 48.8 mmol) was added followed by the dropwise addition of BF$_3$.Et$_2$O (0.2 mL, 1.6 mmol). The reaction mixture was stirred overnight at 25 °C and then *p*-chloranil (5.1 g, 20.7 mmol) was added and stirring continued at 25 °C for 24 h. The reaction mixture was concentrated *in vacuo* and the crude residue obtained was purified by a silica gel column chromatography using CH$_2$Cl$_2$/petroleum ether (3:7 to 2:3 as eluent) to afford the compound **6** (1.2 g, 14.6%) as a purple solid. TLC (CH$_2$Cl$_2$/Hexane, 1:1): R$_f$ = 0.28. ^{1}H NMR (CDCl$_3$): δ = 8.92–8.94 (m, 6H, *β*-pyrrole-C*H*), 8.85 (d, *J = 4 Hz*, 2H, *β*-pyrrole-C*H*), 8.49 (d, *J = 8 Hz*, 2H, R-COTPC-phenyl-*Hm*), 8.36 (d, *J = 8 Hz*, 2H, R-NHTPC-phenyl-*Ho*), 8.26–8.28 (m, 6H, triphenyl-*Ho*), 7.76–7.83 (m, 9H, triphenyl-*Hm,p*), 4.15 (s, 3H, OC*H$_3$*), −2.68 (br s, 2H, α-pyrrole-N*H*) ppm. ^{13}C NMR (CDCl$_3$): δ = 167.49, 147.22, 142.20, 134.69, 131.38, 129.72, 129.65, 128.06, 127.93, 126.86, 120.74, 120.55, 120.31, 118.69, 52.56 ppm. HRMS (ESI): *m/z* calcd for C$_{46}$H$_{33}$N$_4$O$_2$ ([M+H]$^+$), 673.2598; found 673.2581.

5-(4-Carboxyphenyl)-10,15,20-triphenylporphyrin (7) (TPP$_{Cl}$). Compound **6** (1.2 g, 1.78 mmol) was dissolved in a mixture of THF/pyridine (10:1, 100 mL). Then 2N methanolic KOH (120 mL) was added and the reaction mixture was refluxed for 24 h. The reaction mixture was allowed to cool to 25 °C and was then neutralized with a saturated aqueous citric acid solution. Subsequently the reaction mixture was concentrated *in vacuo* to remove the MeOH and THF. The crude residue was then diluted with CH$_2$Cl$_2$ (150 mL) and H$_2$O (120 mL) and the aqueous phase was extracted with CH$_2$Cl$_2$ (3 × 50 mL). The combined organic phase was washed with water (2 × 40 mL) and brine (35 mL), dried over Na$_2$SO$_4$, and concentrated *in vacuo*. The crude product was purified by

a silica gel column chromatography using MeOH/CH$_2$Cl$_2$ (0:100 to 4:96 as eluent) to afford the

acid compound **7** (0.83 g, 71%) as a purple solid. TLC (CH$_2$Cl$_2$/MeOH, 95:5): R$_f$ = 0.54. ^{1}H

NMR (DMSO-d_6): δ = 8.84 (br s, 8H, β-pyrrole-CH), 8.33–8.39 (m, 4H, R-COTPP-phenyl-

Ho,m), 8.21–8.23 (m, 6H, triphenyl-Ho), 7.81–7.88 (m, 9H, triphenyl-Hm,p), −2.92 (s, 2H, α-

pyrrole-NH). HRMS (ESI): m/z calcd for C$_{45}$H$_{31}$N$_4$O$_2$ ([M+H]$^+$), 659.2442; found 659.2446.

5-(4-Carboxyphenyl)-10,15,20-triphenylchlorin (8) (TPC$_{Cl}$). Compound **7** (600 mg, 0.9 mmol)

and anhydrous K$_2$CO$_3$ (1.13 g, 8.2 mmol) were dissolved in pyridine (42 mL) under N$_2$ and

protected from light. p-toluenesulfonyl hydrazide (340 mg, 1.8 mmol) was then added to the

reaction mixture and stirred with heating under reflux. Additional quantities of p-toluenesulfonyl

hydrazide (340 mg, 1.8 mmol) in 3mL of pyridine were added after the periods of 2, 4, 6, 8 and

10 h, and stirring continued under reflux for 24 h. The reaction mixture was then allowed to cool

down to 25 °C before it was poured into EtOAc/H$_2$O (2:1, 750 mL) and again stirred under reflux

for 1 hour. After that it was cooled to 25 °C, the organic phase was separated and washed with 2

N HCl (2 × 150 mL), followed by washing with H$_2$O (2 × 150 mL), dried over Na$_2$SO$_4$ and

concentrated *in vacuo* to give 565 mg of the crude compound. Analysis of the UV-vis spectrum

of the crude revealed that it was the mixture of chlorin and bacteriochlorin (band at 651 nm and

738 nm respectively). Furthermore, analysis by ^{1}H NMR spectra confirmed that there was no

trace amount of starting porphyrin material left unreacted.

The above crude material (chlorin/bacteriochlorin mixture, 565 mg) was completely

dissolved in a 40 ml mixture of CH$_2$Cl$_2$/MeOH (3:1) under N$_2$. To this solution, o-chloranil (180

mg, 0.7 mmol) was added in one portion at 25 °C, and the progress of the reaction monitored

simultaneously by UV-vis. As soon as the absorption peak of bacteriochlorin (738 nm)

diminished, the reaction mixture was quenched with a solid NaHSO$_3$, followed by a washing of

the organic phase with 5% aqueous $NaHSO_3$ (2 × 150 mL), H_2O (100 mL) and 5% aqueous

NaOH (2 × 150 mL) and finally, again with H_2O (120 mL). The emulsion that formed during the

extraction process was removed by washing the organic phase with the saturated aqueous citric

acid solution. The organic phase was dried over Na_2SO_4, filtered and concentrated *in vacuo* to

give exclusively the *chlorin* compound **8** (420 mg, 70%) as a brown solid. *Compound 8 and its*

derivatives exist in two isomeric forms (confirmed by HPLC). TLC (CH_2Cl_2/MeOH, 95:5): $R_f =$

0.54. ^{1}H NMR (DMSO-d_6): δ = 7.91–8.58 (m, 16H, *β*-pyrrole-C*H*, triphenyl-*Ho* & R-COTPC-

phenyl-*Ho,m*), 7.68–7.77 (m, 9H, triphenyl-*Hm,p*), 4.12–4.13 (m, 4H, *chlorin β*-pyrrole-C*H₂*),

−1.53 and −1.60 (br s, 2H, α-pyrrole-N*H*) ppm. ^{1}H NMR ($CDCl_3$): δ = 7.87–8.60 (m, 16H, *β*-

pyrrole-C*H*, triphenyl-*Ho* & R-COTPC-phenyl-*Ho,m*), 7.64–7.74 (m, 9H, triphenyl-*Hm,p*), 4.16–

4.18 (m, 4H, *chlorin β*-pyrrole-C*H₂*), −1.39 and −1.49 (2 br s, 2H, α-pyrrole-N*H*) ppm. HRMS

(ESI) calcd for $C_{45}H_{33}N_4O_2$ ([M+H][+]), 661.2598; found 661.2612.

N-(tert-Butoxycarbonyl)-piperazine (9) (1-Boc-piperazine). Piperazine (6 g, 69.6 mmol) was

dissolved in CH_2Cl_2 (120 mL) and the solution was cooled to 0 °C. To the reaction mixture,

solution of di-*tert*-butyl dicarbonate (Boc$_2$O) (7.6 g, 34.8 mmol) in CH_2Cl_2 (80 mL) was added

dropwise and the stirring was continued for 24 h. The precipitate formed was filtered off and

washed with CH_2Cl_2 (2 × 20 mL), and the combined filtrate was separated and washed with H_2O

(3 × 40 mL), brine (30 mL), dried over Na_2SO_4 and concentrated *in vacuo* to afford the

compound **5** (6.5 g, 50%) as a white solid. mp: 44–46 °C (lit. mp 46–47 °C); ^{1}H NMR ($CDCl_3$): δ

= 3.32 (t, *J = 4 Hz*, 4H), 2.74 (t, *J = 4 Hz*, 4H), 1.60 (s, 1H, N*H*), 1.39 (s, 9H) ppm. ^{13}C NMR

($CDCl_3$): δ = 154.85, 80.00, 79.52, 45.96, 44.45, 28.45 ppm. MS (ESI): *m/z* calcd for $C_9H_{19}N_2O_2$

([M+H][+]), 187.1441; found 187.1434.

5-(4-(4-tert-Butoxycarbonylpiperazin-1-yl)carbonylphenyl)-10,15,20-triphenylchlorin *(10)*. The chlorin compound **8** (500 g, 0.76 mmol) and *tert*-butyl piperazine-1-carboxylate **9** (155 mg, 0.83 mmol) were dissolved in DMF (4 mL) under N_2 and protected from light. *N*-(3-dimethylaminopropyl)-N′-ethylcarbodiimide hydrochloride (EDCI·HCl) (174 mg, 0.91 mmol) and 1-hydroxybenzotriazole hydrate (HOBt) (123 mg, 0.91 mmol) were added to the reaction mixture, followed by an addition of Et_3N (0.26 mL, 1.82 mmol). The reaction mixture was stirred overnight at 25 °C before it was slowly poured into stirring H_2O (100 mL). The solid obtained was filtered off, washed with plenty of H_2O, dried, and then the crude product was purified by a silica gel column chromatography (CH_2Cl_2/MeOH, 100:0 to 99:1 as eluent) to afford the compound **10** (340 mg, 54%) as a brown solid. TLC (CH_2Cl_2/MeOH, 99:1): R_f = 0.74. ^{1}H NMR ($CDCl_3$): δ = 7.74–8.59 (m, 16H, *β*-pyrrole-C*H*, triphenyl-*Ho* & R-COTPC-phenyl-*Ho,m*), 7.65–7.72 (m, 9H, triphenyl-*Hm,p*), 4.16–4.17 (m, 4H, *chlorin β*-pyrrole-C*H₂*), 3.78–3.86 (br m, 4H, piperazine ring-C*H₂*), 3.63 (br m, 4H, piperazine ring-C*H₂*), 1.53 (s, 9H, Boc (C*H₃*)₃), −1.39 and −1.47 (br s, 2H, α-pyrrole-N*H*) ppm.

5-(4-(1-piperazinyl)carbonylphenyl)-10,15,20-triphenylchlorin *(11)* *(TPC$_{C1P}$)*. The compound **10** (320 mg, 0.39 mmol) was dissolved in CH_2Cl_2 (8 mL) under N_2 and with protection from light. To this solution TFA/CH_2Cl_2 (1:1, 4 mL) was added and the reaction mixture was stirred at 25 °C for 1 h, before it was diluted with CH_2Cl_2 (40 mL), and the organic phase was washed with H_2O (2 × 15 mL), saturated aqueous $NaHCO_3$ (2 × 15 mL), and brine (15 mL). The organic phase was then dried over Na_2SO_4 and concentrated *in vacuo*. The crude residue was then purified by a silica gel column chromatography (CH_2Cl_2/MeOH, 100:0 to 92:8 as eluent) to afford the key intermediate compound **11** (250 mg, 89%) as a brown solid. TLC (CH_2Cl_2/MeOH, 9:1): R_f = 0.35. ^{1}H NMR ($CDCl_3$): δ = 7.74–8.59 (m, 16H, *β*-pyrrole-C*H*, triphenyl-*Ho* & R-COTPC-

phenyl-*Ho,m*), 7.64–7.72 (m, 9H, triphenyl-*Hm,p*), 4.16–4.17 (m, 4H, *chlorin β*-pyrrole-C*H₂*), 3.73–3.90 (br m, 4H, piperazine ring-C*H₂*), 3.04 (br m, 4H, piperazine ring-C*H₂*), −1.40 and −1.47 (br s, 2H, α-pyrrole-N*H*) ppm. HRMS (ESI): calcd for $C_{49}H_{41}N_6O$ ([M+H]$^+$), 729.3336; found 729.3332.

Chitosan mesylate (12). This compound was synthesized according to our previously published procedure.[37] FT-IR (KBr): ν = 3342 (br, O–H), 3312, 3052, 3022, 2816 (m, C–H), 1691 (vs, C=O amide I), 1596 (vs, C=O amide II), 1557, 1471, 1439, 1400, 13408, 1178, 965, 799, 700 cm^{-1}. ^{1}H NMR (D₂O): δ = 4.86 (H-1, partly overlapped with HDO peak), 3.73–3.92 (m, *H-2* GlcNAc, *H-3*, *H-4*, *H-5*, *H-6*, *H-6´*), 3.18 (m, *H-2* GlcN), 2.81 (s, C*H₃*S), 2.06 (s, C*H₃*CO) ppm. ^{1}H NMR (DMSO-d_6): δ = 8.26 (br s, 2H), 5.38–4.80 (m, 3H), 3.50–3.71 (m, 4H), 2.87 (br s, 1H), 2.42 (s, 3H) ppm. ^{13}C NMR (D₂O): δ = 100.09, 78.84, 77.28, 72.62, 62.49, 58.32, 41.05, 13.80 ppm. ^{13}C NMR (DMSO-d_6): δ = 97.73, 77.80, 74.90, 70.22, 60.39, 55.83 ppm.

3,6-Di-O-tert-butyldimethylsilyl-chitosan (13) (Di-TBDMS-chitosan). This compound was synthesized according to our previously published procedure.[37] FT-IR (KBr): ν = 2957, 2931, 2886, 2858 (s, C–H, TBDMS), 1474, 1390, 1362, 1258, 108, 1005, 836, 777 (Si–C), 670 cm^{-1}. ^{1}H NMR (CDCl₃) δ: 4.30 (br s, *H-1*), 3.89 and 3.85 (br s, *H-6*, *H-6'*), 3.68 (br s, *H-4*), 3.50 (br s, *H-3*), 3.33 (br s, *H-5*), 2.72 (br s, *H-2* GlcN), 0.90 and 0.89 (br s, (C*H₃*)₃C-Si), 0.13, 0.10, 0.06, 0.05 (br s, (C*H₃*)₂Si) ppm.

N-bromoacetyl-3,6-di-O-tert-butyldimethylsilyl-chitosan (14) (BrA-Di-TBDMS-chitosan). Silyl compound **13** (1 g, 2.60 mmol) was dissolved in dry CH_2Cl_2 (15 mL) under N₂ atmosphere. This solution was cooled to a −20 °C by using an ice/salt mixture and then Et₃N (1.81 mL, 13 mmol) was added, followed by a slow dropwise addition of bromoacetyl bromide (0.91 mL, 10 mmol).

20

The stirring was continued for exactly 1 h at -20 °C, before the reaction mixture was diluted with CH$_2$Cl$_2$ (40 mL) and concentrated *in vacuo*. The obtained crude residue was triturated and stirred with CH$_3$CN (30 mL), filtered and washed with fresh CH$_3$CN (3 × 15 mL) and dried. The dry material was dissolved in CH$_2$Cl$_2$ and the organic phase was washed with H$_2$O (3 × 30 mL) and brine (25 mL), dried over Na$_2$SO$_4$, and concentrated *in vacuo* to afford the bromoacetyl compound **14** (1.2 g, 92%) as a faint yellow powder. FT-IR (KBr): ν = 3402 (br , NH), 2957, 2931, 2886, 2858 (s, C–H, TBDMS), 1682 (vs, C=O amide I), 1530 (vs, C=O amide II), 1473, 1391, 1362, 1311, 1259, 1101, 1005, 837, 777 (Si–C), 669 cm^{-1}; ^{1}H NMR (CDCl$_3$) δ = 4.40 (br s, *H-1*), 4.02–3.26 (m, *H-2* GlcN, *H-3*, *H-4*, *H-5*, *H-6*, *H-6'* and GlcNHCOC*H$_2$*Br), 0.90 and 0.88 (br s, (C*H$_3$*)$_3$C-Si), 0.13 and 0.07 (br s, (C*H$_3$*)$_2$Si) ppm.

[N-(2-(4-(N-(4-(10,15,20-triphenylchlorin-5-yl)phenylamino)carbonylmethyl)piperazin-1-yl)acetyl)]$_{0.1}$[N-(2-bromoacetyl)]$_{0.9}$-3,6-di-O-tert-butyldimethylsilyl-chitosan

(15) (TPC$_{NIP}$)$_{0.1}$(Br)$_{0.9}$-A-Di-TBDMS-chitosan). The chitosan intermediate **14** (800 mg, 1.58 mmol) and the amino-chlorin intermediate **4** (TPC$_{NIP}$) (120 mg, 0.158 mmol) were dissolved in CH$_2$Cl$_2$ (25 mL) under N$_2$ and with protecion from light. An exact equimolar quantity of Et$_3$N (22 μL, 0.158 mmol) with respect to **4** was added and the reaction mixture was stirred at 25 °C for 24 h. The full consumption of the starting material was confirmed by TLC. The reaction mixture was diluted with CH$_2$Cl$_2$ (55 mL) and washed with H$_2$O (2 × 25 mL) and brine (25 mL). The organic phase was dried over Na$_2$SO$_4$, and concentrated *in vacuo* to afford compound **15** (700 mg, 78%) as a brown solid. ^{1}H NMR (CDCl$_3$): δ = 9.21, 9.25 (s, TPC-N*H*CO), 7.86–8.60 (m, *β*-pyrrole-C*H*, triphenyl-*Ho* & R-NHTPC-phenyl-*Ho,m*), 7.65–7.73 (m, triphenyl-*Hm,p*), 3.35–4.50 [br m, chitosan (*H-1*, *H-2* GlcN, *H-3*, *H-4*, *H-5*, *H-6*, *H-6'* and *H-2* GlcNAc, C*H$_2$*CONHGlc), TPC-NHCOC*H$_2$*-pip, piperazine ring-C*H$_2$* and *chlorin β*-pyrrole-C*H$_2$*], 2.77–2.83 (m, piperazine

ring-CH_2), 0.88–0.89 [br s, (CH_3)$_3$C-Si], 0.02–0.13 [(br m, (CH_3)$_2$Si], −1.44 (br s, 2H, α-pyrrole-NH).

[N-(2-(4-(4-(10,15,20-triphenylchlorin-5-yl)phenylcarbonyl)piperazin-1-yl)acetyl)]$_{0.1}$[N-(2-bromoacetyl)]$_{0.9}$-3,6-di-O-tert-butyldimethylsilyl-chitosan (20) ((TPC$_{C1P}$)$_{0.1}$(Br)$_{0.9}$-A-Di-TBDMS-chitosan). The chitosan intermediate **14** (800 mg, 1.58 mmol) was dissolved in *N*-Methyl-2-pyrrolidone (NMP) (15 mL) under N$_2$ and with protection from light. The carboxyl-chlorin intermediate **11** (TPC$_{C1P}$) (125 mg, 0.173 mmol), and NaHCO$_3$ (0.29 g, 3.45 mmol) were added and the reaction mixture was heated to 75 °C and stirred overnight, before it was cooled to 25 °C, and poured into stirring H$_2$O. The obtained crude solid was filtered off, washed with plenty of H$_2$O and dried. The crude material was dissolved in CH$_2$Cl$_2$, washed with H$_2$O (2 × 25 mL and brine (25 mL), filtered, dried over Na$_2$SO$_4$, and concentrated *in vacuo* to obtain the compound **20** (810 mg, 89%) as a brown solid. ^{1}H NMR (CDCl$_3$): δ = 7.75–8.60 (m, *β*-pyrrole-CH, triphenyl-*Ho* and R-COTPC-phenyl-*Ho,m*), 7.64–7.71 (m, 9H, triphenyl-*Hm,p*), 3.38–4.5 [br m, chitosan (*H-1*, *H-2* GlcN, *H-3*, *H-4*, *H-5*, *H-6*, *H-6'* and *H-2* GlcNAc, CH_2CONGlc), piperazin ring-CH_2 and *chlorin β*-pyrrole-CH_2], 2.76–2.84 (m, piperazin ring-CH_2), 0.89–0.92 [br s, (CH_3)$_3$C-Si], 0.02–0.10 [(br m, (CH_3)$_2$Si)], −1.40 and −1.48 (br s, 2H, α-pyrrole-NH) ppm.

General Procedure <u>A</u> for the Synthesis of Compounds 16 and 21.

[N-(2-(4-(N-(4-(10,15,20-triphenylchlorin-5-yl)phenylamino)carbonylmethyl)piperazin-1-yl)acetyl)]$_{0.1}$[N-(2-(N,N,N-trimethylammoniumyl)acetyl)]$_{0.9}$-3,6-di-O-tert-butyldimethylsilyl-chitosan bromide (16) (TPC$_{N1P}$)$_{0.1}$-Di-TBDMS-chitosan-TMA. Compound **15** (350 mg, 0.61 mmol) was dissolved in CH$_2$Cl$_2$ (15 mL) under N$_2$ and with protection from light. Excess Me$_3$N (31–35 wt % in EtOH, 4.2 M) (15 mL) solution was added to the reaction mixture and it was stirred at 25 °C for 24 h. The reaction mixture was concentrated *in vacuo* and the crude material

22

was completely dried under high vacuum, yielding the crude compound **16** (355 mg) as a brown

solid. The material **16** was used directly for the next step without further purification.

[N-(2-(4-(4-(10,15,20-triphenylchlorin-5-yl)phenylcarbonyl)piperazin-1-yl)acetyl)]$_{0.1}$[N-(2-

(N,N,N-trimethylammoniumyl)acetyl)]$_{0.9}$-3,6-di-O-tert-butyldimethylsilyl-chitosan bromide (21)

(TPC$_{C1P}$)$_{0.1}$-Di-TBS-chitosan-TMA. The general procedure *A* was followed using **20** (350 mg,

0.61 mol) and trimethylamine solution to give **21** as crude solid (360 mg), which was used

without further purification for the next step.

General Procedure B for the Synthesis of Compounds 17 and 22.

[N-(2-(4-(N-(4-(10,15,20-triphenylchlorin-5-yl)phenylamino)carbonylmethyl)piperazin-1-

yl)acetyl)]$_{0.1}$-[N-(2-(4-methylpiperazin-1-yl)acetyl)]$_{0.9}$-3,6-di-O-tert-butyldimethylsilyl-chitosan

(17) (TPC$_{N1P}$)$_{0.1}$-Di-TBDMS-chitosan-MP. Compound **15** (350 mg, 0.61 mmol) was dissolved in

CH$_2$Cl$_2$ (15 mL) under N$_2$ and with protection from light. Excess of 1-methylpiperazine (10 mL)

was added to the reaction mixture that was stirred at 25 °C for 24 h. The reaction mixture was

concentrated *in vacuo* and the crude product was completely dried under high vacuum yielding

the corresponding crude product **17** (330 mg), which was used without further purification for the

next step.

[N-(2-(4-(4-(10,15,20-triphenylchlorin-5-yl)phenylcarbonyl)piperazin-1-yl)acetyl)]$_{0.1}$[N-(2-(4-

methylpiperazin-1-yl)acetyl)]$_{0.9}$-3,6-di-O-tert-butyldimethylsilyl-chitosan (22) (TPC$_{C1P}$)$_{0.1}$-Di-

TBDMS-chitosan-MP. The general procedure *B* was followed using the compound **20** (250 mg,

0.38 mol) and 1-methylpiperazine to yield the compound **22** (265 mg) as a crude solid, which

was used as it is for the next step.

Final TBDMS-deprotection was carried out by following general procedure C.

Synthesis of the TPC-chitosan nano-conjugates (18, 19, 23 and 24).

The compound (**16**, **17**, **21**, **22**) was dissolved in MeOH (20 mL) under N_2 and the reaction mixture was protected from light. The reaction mixture was degassed by purging it with N_2 for 5 minutes and subsequently cooled to 0 °C, before the addition of concd HCl (4 mL). The reaction mixture was allowed to warm up to 25 °C and stirred for 12 h. The reaction mixture was then diluted and ion-exchanged by the addition of 5% NaCl (aqueous) (40 mL) to the solution. It was then stirred for 1 h before it was dialyzed against 8% NaCl (aqueous) for 24 h, and then again against deionized water for two days. The clean brown solution was subsequently freeze dried to afford the corresponding final nano-conjugates (**18**, **19**, **23**, **24**) as a brown fluffy material. *Sometimes the reaction needed to be repeated in order to get rid of a trace amount of TBDMS that was left un-deprotected from the chitosan backbone.*

[N-(2-(4-(N-(4-(10,15,20-triphenylchlorin-5-yl)phenylamino)carbonylmethyl)piperazin-1-yl)acetyl)]$_{0.1}$[N-(2-(N,N,N-trimethylammoniumyl)acetyl)]-chitosan chloride (18) [(TPC$_{N1P}$)$_{0.1}$-CS-TMA]. The general procedure *C* was followed by using compound **16** (325 mg, 0.52 mmol) and concd HCl/MeOH to afford the nano-conjugate **18** (175 mg, 85%) as a brown solid. ^{1}H NMR (DMSO-d_6/D$_2$O, 96:4): δ = 7.83–8.62 (m, *β*-pyrrole-C*H*, triphenyl-*Ho* & R-NHTPC-phenyl-*Ho,m*), 7.69–7.77 (m, triphenyl-*Hm,p*), 4.52 (br s, *H-1*), 4.11–4.14 (m, C*H₂*CONGlc and *chlorin β*-pyrrole-C*H₂*), 3.26–3.67 (br m, partially overlapped with HDO peak, *H-2* GlcNAc, *H-3*, *H-4*, *H-5*, *H-6*, *H-6′*, *H-2* GlcNHCO, TPCNHCOC*H₂*-pip, piperazine ring-C*H₂*), 3.24 (s, $^+$N(C*H₃*)$_3$)) ppm. UV-vis (DMSO): λ$_{max}$ = 421, 520, 549, 599, 651 nm.

[N-(2-(4-(N-(4-(10,15,20-triphenylchlorin-5-yl)phenylamino)carbonylmethyl)piperazin-1-yl)acetyl)]$_{0.1}$-[N-(2-(4-methylpiperazin-1-yl)acetyl)]-chitosan (19) [(TPC$_{N1P}$)$_{0.1}$-CS-MP]. The general procedure *C* was followed by using compound **17** (300 mg, 0.45 mmol) and concd

HCl/MeOH to afford the nano-conjugate **19** (165 mg, 84%) as a brown solid. ^{1}H NMR (DMSO-d_6/D_2O, 96:4): δ = 7.83–8.62 (m, *β*-pyrrole-C*H*, triphenyl-*Ho* & R-NHTPC-phenyl-*Ho,m*), 7.66–7.75 (m, triphenyl-*Hm,p*), 4.50 (br s, *H-1*), 4.10–4.14 (m, *chlorin β*-pyrrole-C*H₂*), 2.92–3.55 (m, partially overlapped with HDO peak , *H-2* GlcNAc, *H-3*, *H-4*, *H-5*, *H-6*, *H-6′*, *H-2* GlcNHCO, C*H₂*CONGlc, TPCNHCOC*H₂*-pip), 2.33–2.63 (m, partially overlapped with DMSO-d_6 peak, piperazine ring-C*H₂*, piperazine-N-C*H₃*) ppm. UV-vis (H_2O): λ_{max} = 412, 430, 531, 560, 611, 664 nm. UV-vis (DMSO): λ_{max} = 421, 521, 548, 596, 651 nm.

[N-(2-(4-(4-(10,15,20-triphenylchlorin-5-yl)phenylcarbonyl)piperazin-1-yl)acetyl)]₀.₁[N-(2-(N,N,N-trimethylammoniumyl)acetyl)]-chitosan chloride (23) [(TPC_{C1P})₀.₁-CS-TMA]. The general procedure *C* was followed using the compound **21** (300 mg, 0.48 mmol) and concd HCl/MeOH to afford the nano-conjugate **23** (170 mg, 89%) as a brown solid. FT-IR (KBr): ν = 3353, 3061, 2950, 1683, 1580, 1473, 1440, 1376, 1291, 1154, 1112, 1067, 1032, 970, 911, 794, 703 cm^{−1}. ^{1}H NMR (DMSO-d_6/D_2O, 96:4): δ = 7.89–8.62 (m, *β*-pyrrole-C*H*, triphenyl-*Ho* & R-COTPC-phenyl-*Ho,m*), 7.67–7.76 (m, triphenyl-*Hm,p*), 4.50 (br s, *H-1*), 4.06–4.16 (m, C*H₂*CONGlc and *chlorin β*-pyrrole-C*H₂*), 3.26–3.75 (m, partially overlapped with HDO peak, *H-2* GlcNAc, *H-3*, *H-4*, *H-5*, *H-6*, *H-6′*, *H-2* GlcNHCO, piperazine ring-C*H₂*), 3.24 (s, [+]N(C*H₃*)₃)) ppm. UV-vis (DMSO): λ_{max} = 420, 520, 547, 599, 651 nm.

[N-(2-(4-(4-(10,15,20-triphenylchlorin-5-yl)phenylcarbonyl)piperazin-1-yl)acetyl)]₀.₁[N-(2-(4-methylpiperazin-1-yl)acetyl)]-chitosan (24) [(TPC_{C1P})₀.₁-CS-MP]. The general procedure *C* was followed using the compound **22** (240 mg, 0.38 mmol) and concd HCl/MeOH to afford the compound **24** (85 mg, 52%) as a brown solid. FT-IR (KBr): ν = 3349, 2927, 1644, 1580, 1461, 1440, 1374, 1285, 1070, 1043, 985, 945, 794, 719, 703 cm^{−1}. ^{1}H NMR (DMSO-d_6/D_2O, 96:4): δ = 7.86–8.63 (m, *β*-pyrrole-C*H*, triphenyl-*Ho* & R-COTPC-phenyl-*Ho,m*), 7.67–7.76 (m,

triphenyl-*Hm,p*), 7.69–7.80 (m, triphenyl-*Hm,p*), 4.50 (br s, *H-1*), 4.08–4.14 (m, *chlorin β-pyrrole*-CH_2), 2.92–3.55 (m, partially overlapped with HDO peak, *H-2* GlcNAc, *H-3*, *H-4*, *H-5*, *H-6*, *H-6′*, *H-2* GlcNHCO, CH_2CONGlc), 2.27–2.63 (m, partially overlapped with DMSO-d_6 peak, piperazine ring-CH_2, piperazine N-CH_3) ppm. UV-vis (DMSO): λ_{max} = 421, 520, 547, 599, 651 nm.

Porphyrin (TPP) analogues of 18, 19, 23 and 24.

Unexpected results (back-oxidation of TPC-chitosan nano-conjugates to their TPP analogue nano-conjugates by TBAF/NMP) were observed when the following general TBDMS-deprotection procedure *D* was followed:

Example: TPP analogue of nano-conjugate 18.

[N-(2-(4-(N-(4-(10,15,20-triphenylporphyrin-5-yl)phenylamino)carbonylmethyl)piperazin-1-yl)acetyl)]$_{0.1}$[N-(2-(N,N,N-trimethylammoniumyl)acetyl)]-chitosan chloride [(TPP$_{N1P}$)$_{0.1}$-CS-TMA]. The compound **16** (600 mg, 0.86 mmol) was dissolved in NMP (5–10 mL) at 55 °C under N$_2$ atmosphere and protected from light. Excess amount of *tetra-n*-butyl ammonium fluoride (TBAF) was added to the reaction mixture and the stirring continued for 24 h at 55 °C. The reaction mixture was cooled to 25 °C, diluted and ion exchanged with the 5% NaCl (aqueous, 40 mL) for 1 hour. The solution was then dialyzed against 8% NaCl (aqueous) for 24 h, and then again against deionized water for two days. The red colored solution was then freeze-dried to yield purple colored sponge-like material. Surprisingly, after analysis, it was established that due to back-oxidation the chlorin compounds were converted back to their TPP analogues that were confirmed by ^{1}H NMR and UV-vis (as the characteristic peak at 650 vanished) *(Data not shown)*.

Biological Studies

Materials

The HCT116/LUC human colon carcinoma cell line (permanently transfected with a gene encoding luciferase) was kindly provided by Dr. Mohammed Amarzguioui, siRNAsense, Oslo, Norway. MTT [3-(4,5-Dimethylthiazol-2-yl)-2,5-diphenyltetrazolium bromide] was from Sigma-Aldrich (MO, U.S.; cat. no. M 2128), and was dissolved in phosphate-buffered saline (PBS) to a concentration of 5 mg/mL, sterile filtered and stored at 4 °C. A plasmid encoding enhanced green fluorescent protein (pEGFP-N1) was purchased from Clontech Laboratories Inc. (CA, U.S.; Cat. No. 6085-1), produced by ELIM Biopharmaceuticals, Inc. (CA, U.S.) (lot# 1002) and delivered at a concentration of 2 mg/mL in sterile water. This stock solution was aliquoted and kept at −20 °C. Poly-L-Lysine hydrobromide (Mw 15–30 kDa) was purchased from Sigma-Aldrich (MO, U.S.; cat. no. P 7890). Poly-L-Lysine hydrobromide was dissolved and diluted in distilled water, sterilized by filtration and stored at –20 °C.

In Vitro Cell Culture Studies

Cell Cultivation. HCT116/LUC were cultured in Dulbecco's Modified Eagle's Medium (DMEM) (Lonza, Veviers, Belgium), supplemented with 10% fetal calf serum (PAA Laboratories GmbH, Pasching, Austria) 100 U/mL penicillin and 100 µg/mL streptomycin (Sigma-Aldrich, MO, U.S.) at 37 °C and 5% CO_2 in a humid environment.

Treatment of the Cells. HCT116/LUC cells (1.5×10^5 cells per well for the transfection expriments, 3.75×10^5 cells per well for the MTT assay) were seeded into 6-well (transfection) and 24-well (MTT) plates (Nunc, Roskilde, Denmark) and incubated for 24 h (5% CO_2, 37 °C).

27

The photosensitizer TPCS$_{2a}$ or the TPC-chitosan nano-conjugates (**18**, **19**, **23**, and **24**) were then added to the cells and the cells were incubated for 18 h (5% CO_2, 37 °C). The cells were then washed three times with the cell culture medium and incubated for 4 h (5% CO_2, 37 °C) in a medium containing the plasmid complex. The cells were washed once and after the addition of fresh medium, the cells were illuminated with different light doses. After 48 h of incubation, the expression of EGFP (Enhanced Green Fluorescent Protein) was analyzed by flow cytometry. Cell survival was measured by the MTT assay in parallel experiments.

The cells were exposed to light from LumiSource® (PCI Biotech, Oslo, Norway). LumiSource® is delivered with a bank of 4 light tubes (4 × 18 W Osram L 18/67, Blue) emitting mainly blue light with a peak wavelength in the region of 420–435 nm and an irradiance of 13 mW/cm^2.

Preparation of Plasmid/poly-L-lysine Complexes. Plasmid/poly-L-lysine complexes with a charge ratio of 2.2:1 (charge ratio is: (number of positive charges (primary amines) in poly-L-lysine)/number of negative charges in the phosphate groups of the DNA) were formed by the gentle mixing of plasmid DNA and poly-L-lysine solutions. 2.5 µl of DNA (stock solution 2 µg/µL) was diluted with 47.5 µL water, and 6.92 µl poly-L-lysine (1 µg/µL) was diluted with 43.08 µL water. After mixing, the solution was incubated at 25 °C for 30 min, then diluted with the culture medium to a final volume of 1 mL and added to the cells (1 mL per well).

Measurement of Transfection. The cells were trypsinized in 100 µL trypsin (Trypsin- EDTA, Sigma-Aldrich, MO, U.S.), re-suspended in a 500 µL cell culture medium and filtered through a 5 mL Polystyrene Round-Bottom Tube with a Cell-Strainer Cap (BD Falcon) (50 µm mesh nylon filter) before analysis in a BD LSR flow cytometer (Becton Dickinson, CA, U.S.). EGFP was measured through a 500-550 nm filter after excitation at 450-490 nm, and the propidium iodide

28

(Calbiochem Corporation, CA, U.S.) was measured through a 600–620 nm filter after excitation at 561 nm. Propidium iodide (1 μg/mL) was used to discriminate dead cells from viable cells and pulse-processing was performed to discriminate cell doublets from single cells. 10,000 events were collected for each sample and the data was analyzed with BD FACSDiva Software (Becton Dickinson, CA, U.S.).

Measurement of Cell Survival. Cell survival was measured by a method based on the reduction of a water-soluble tetrazolium salt (MTT) to a purple, insoluble formazan product by the mitochondrial dehydrogenases present in living, metabolically active cells. 0.5 mL medium containing 0.125 mg MTT was added to the cells, followed by a 2 h incubation at 37 °C, 5% CO_2. The resulting formazan crystals were dissolved by adding 500 μL DMSO (Sigma-Aldrich, MO, U.S.) per well. The plates were read by a PowerWave XS2 Microplate Spectrophotometer (Bio-Tek Instruments, VT, U.S.). Cell survival was calculated as the percent of controls (parallels with no light).

In Vivo **Studies**

Animals. Hsd:Athymic nude-*Foxn1^{nu}* female mice were bred at the animal department at the Norwegian Radium Hospital. The mice were kept under specific pathogen-free conditions. Water and food was given *ad libitum*. All procedures involving mice were carried out in agreement with protocols approved by the animal care committee at the Norwegian Radium Hospital, following the National Ethical Committee's guidelines on animal welfare.

The six mice were 22–25 g (5–8 weeks old) when included in the experiment. The HCT116/LUC cells were cultured at 37 °C and 5% CO_2 in a humid environment before transplantation. 1.5×10^6 cells were injected subcutaneously on the right hip of each mouse.

29

Treatment. The TPC-chitosan nano-conjugates were diluted to a TPC concentration of 1.25 mg/mL in PBS (compound **23**) and 3% Tween 80 (compounds **24** and **19**). 88–100 μL was injected intravenously in the tail vein (final dose 5 mg/kg) when the tumors had reached a volume of 60–100 mm^3. The TPCS$_{2a}$ was diluted to 1.25 mg/mL in 3% Tween 80 and 88–100 μL was injected intravenously in the tail vein (final dose 5 mg/kg) when the tumors had reached a volume of 60–100 mm^3. 96 h after the injection of photosensitizer, the tumors were illuminated with a 652 nm diode laser (Ceramoptec GmbH, Bonn, Germany) at an irradiance of 90 mW/cm^2 and with a 15 J/cm^2 light dose. For animals receiving PCI + Bleomycin treatment, 1500 IU Bleomycin (European units) in 100 μL were injected intraperitoneally. The tumors were illuminated 30 min after the BLM injection as described above. The animals were covered with aluminum foil except the tumor area where a hole was made in the foil that was 2 mm larger in diameter than the tumor area.

In Vivo **Imaging System.** The bioluminescence was measured with an IVIS Lumina 100 Series from Caliper Life Sciences, MA, U.S. The animals were anesthetized (Zoletil) and injected with 200 μL D-Luciferin (Caliper Life Sciences) (20 mg/mL in PBS) intraperitoneally. Images were taken 10 min after the D-Luciferin injection. The bioluminescence was measured approximately once a week from day 11 after the PS injection. The animals were sacrificed when the tumor reached a volume > 1000 mm^3 or when the animal was showing signs of pain or abnormal behavior. The data were analyzed with the Living Image 4.2 Software (Caliper Life Sciences).

RESULTS AND DISCUSSION

Chemistry

In order to explore the biological significance of our previous findings, four amphiphilic chlorin-based TPC-chitosan conjugates were synthesized by utilizing two different PSs which have mono-amino (TPC$_{N1}$) and mono-carboxyl (TPC$_{C1}$) functional groups at the *para*-position of one of the phenyl ring of TPC. The protocol for the efficient synthesis of these PSs (TPC$_{N1}$ and TPC$_{C1}$) was optimized and these pure chlorin PSs then attached to chitosan with 0.10 DS through different synthetic strategies using different linkers and spacer groups, as described below.

Nucleophilic Amino-chlorin Intermediate (TPC$_{N1P}$). Careful consideration in planning of the synthetic strategies are important for chlorin derivatization as these entities could be easily oxidized back to more stable porphyrin analogues, and thus one could easily end up with porphyrin-contaminated products. Therefore, first converting TPP to TPC, and then transforming it into mono-functional amino-derivatives was avoided, as it involved a nitration step, which could have led to oxidation of the ring system to give porphyrin product. Instead, initially mono-amino porphyrin 5-(4-aminophenyl)-10,15,20-triphenylporphyrin (**2**) (TPP$_{N1}$) was synthesized by controlled regioselective nitration of TPP using NaNO$_2$/TFA (1.8 equiv, 3 min), followed by reduction using SnCl$_2$/HCl.[41] Amino-porphyrin **2** was then converted to the corresponding amino-chlorin by the well-known Whitlock diimide reduction method.[42] This is a two-step reduction-oxidation method involving the reduction of one or more pyrrolic β-double bonds by the reaction with diimide generated *in situ* by the thermal decomposition of *p*-toluenesulfonylhydrazide in the presence of base, in refluxing picoline or pyridine solvent. In this process, different reduced porphyrinogen products are theoretically possible (Figure 1), of which the mixture of dihydro (chlorin) and tetrahydro (bacteriochlorin) is mainly formed.
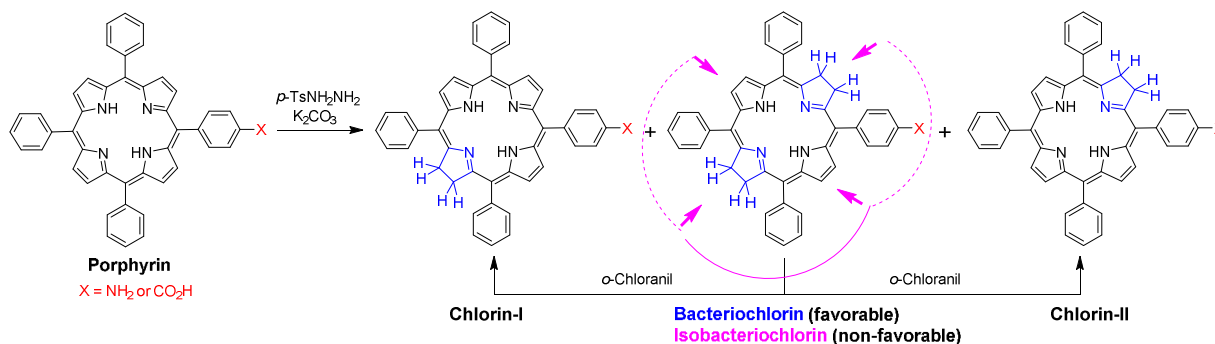
31

Figure 1. Possible formation of corresponding reduced isomers of TPC_{N1} and TPC_{C1} after diimide reduction of porphyrins TPP_{N1} and TPC_{C1}.

In the second oxidation-step, the chlorin compound could be obtained from the mixture by two approaches: (a) by taking advantage of the relative basicity difference of the particular compound from this mixture (porphyrin > chlorin, isobacteriochlorin > bacteriochlorin), which is inversely equal to the strength of phosphoric acid. Therefore, different percentages (w/w) of phosphoric acid (H_3PO_4) in water could be used for the separation of chlorin from the rest of the mixture by utilizing their difference in partition coefficients between benzene and phosphoric acid. (b) The second approach is 3,4,5,6-tetrachloro-1,2-benzoquinone (*o*-chloranil)-mediated dehydrogenation of bacteriochlorin to obtain chlorin.[42] In the literature, other oxidizing agents like MnO_2,[43] and other methodologies using different solvents such as nitrobenzene/acetic acid for controlled back-oxidation,[44] have been reported. Yet, it seems that none have proved to be very effective in producing un-contaminated chlorin derivatives.
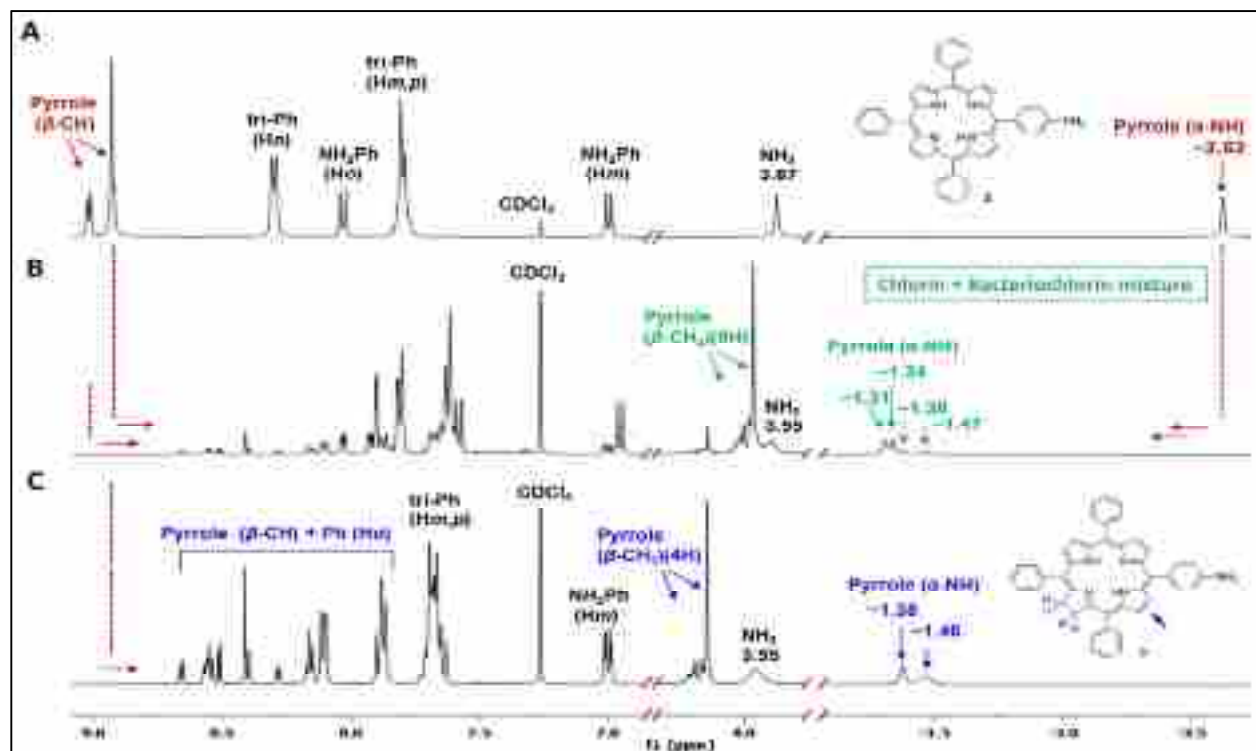
In our synthesis, amino-porphyrin (**2**) was first converted into its reduced mixture using an excess of *p*-toluenesulfonylhydrazide in the presence of K_2CO_3 in refluxing pyridine, after prolonged heating. Initially we tried the earlier-discussed approach-(a), in order to get the pure chlorin compound from the mixture; however, the desired results were not achieved. Furthermore, as all of these compounds have nearly equal R_f values, column chromatographic

separation was not feasible. Therefore, controlled back-oxidation of the chlorin/bacteriochlorin

mixture was the only alternative.

Before going further with back-oxidation, after the first step, the complete consumption of

porphyrin was essentially confirmed by ^{1}H NMR (Figure 2) instead of only relying on the UV-vis

absorption spectrum. This was because UV-vis spectroscopy alone was found to be misleading

when examining whether any trace amount of TPP was left unreacted. Again, although *o*-

chloranil is the most efficient oxidant for the back-oxidation, it needs to be used carefully and in

a controlled manner to avoid over-oxidation which could lead to formation of a porphyrin

contaminant.[45] Hence, the isolated chlorin/bacteriochlorin mixture of **2** was first dissolved in

CH_2Cl_2 completely and then added *o*-chloranil at 25 °C. Initial investigations demonstrated that

the addition of *o*-chloranil (0.8 equiv) in a single portion (instead of portion wise) and the

continuous monitoring of the progress of the reaction by UV-vis spectroscopy just after the

addition of reagent was the key for success. The characteristic peak for bacteriochlorin at 738 nm

decreased and simultaneously the peak at 650 nm for chlorin increased quickly as the reaction

progressed. As soon as the peak at 738 nm was reduced to <0.1 absorbance, the reaction was

quenched by the addition of sodium bisulfite and immediate work-up afforded a pure amino-

chlorin compound 5-(*p*-aminophenyl)-10,15,20-triphenylchlorin (**3**) (TPC_{N1}). In the ^{1}H NMR

analysis, the absence of a peak at –2.68 ppm (for α-pyrrole-N*H*) and 8.92–9.01 ppm (for β-

pyrrole-C*H*) was enough to indicate that there was no trace porphyrin contamination. The [1]H

NMR (Figure 2), HPLC and HRMS analysis (*Supporting Information*) of **3** confirmed that the

pure chlorin compound without any porphyrin contamination was successfully achieved. Also,

UV-vis spectrum analysis showed that the characteristic chlorin Q-(band-I) peak shifted from 646
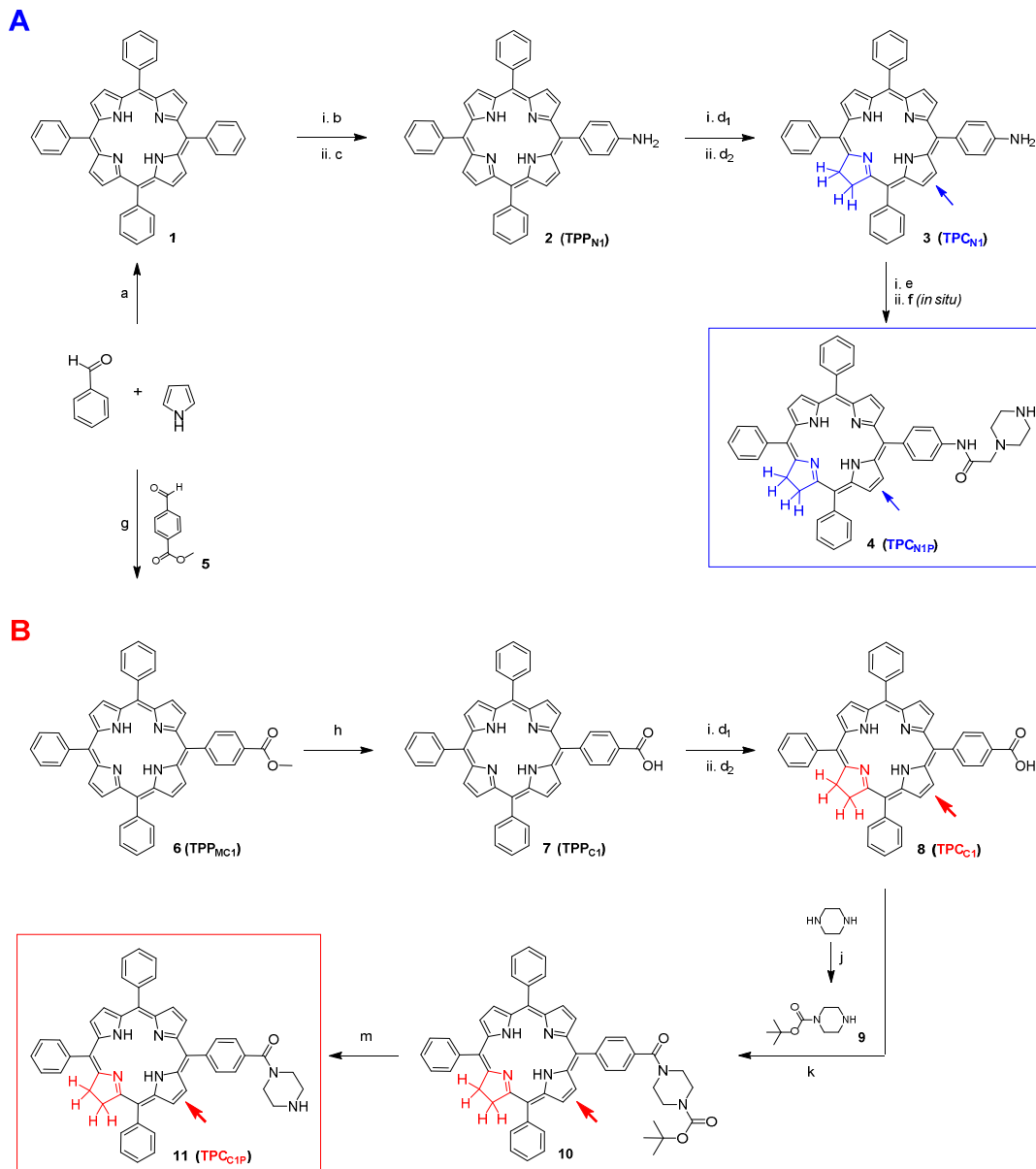
→653 nm along with a > 5-fold increase in the absorption coefficient of this band as compared to

its porphyrin analogue.

The amino-chlorin **3** was then reacted with chloroacetylchloride in the presence of triethylamine in CH$_2$Cl$_2$, followed by an *in situ* nucleophilic attack of excess piperazine at 25 °C. This afforded the strategically key nucleophilic intermediate **4** (TPC$_{N1P}$), which was purified and confirmed by NMR, HR-MS and UV-vis before it could be used for the synthesis of TPC$_{N1P}$-chitosan nano-conjugates **(18** and **19).** ^{1}H NMR analysis of compound **3** showed two peaks for inner pyrrolic-N*H* protons at −1.38 and −1.46 ppm and a single peak at −1.37 for compound **4**. HPLC analysis confirmed that chlorin compounds **3** (in the ratio 1:0.98) and **4** (in the ratio 1:0.86) are present in two isomeric forms, as presumed theoretically (*as shown in* Scheme 1A).

Figure 2. ^{1}H NMR overlay of transformation of the amino-porphyrin to the amino-chlorin: (A) Amino-porphyrin TPP$_{N1}$ (**2**); (B) Chlorin and bacteriochlorin mixture after diimide reduction of **2**; (C) Amino-chlorin TPC$_{N1}$ (**3**).

Scheme 1. Synthesis of the Key Nucleophilic Intermediate **4** (TPC$_{N1P}$) and **11** (TPC$_{C1P}$)

Reagents and conditions: (a) Propionic acid, reflux, 30 min (20%); (b) NaNO$_2$ (1.8 equiv), TFA, 25 °C, 3 min; (c) SnCl$_2$.2H$_2$O, concd HCl, 60 °C, 1 h (54%); (d$_1$) *p*-Toluenesulfonyl hydrazide, K$_2$CO$_3$, pyridine, reflux, 24 h; (d$_2$) *o*-Chloranil, CH$_2$Cl$_2$, 25 °C (80%); (e) Chloroacetyl chloride, Et$_3$N, CH$_2$Cl$_2$, 25 °C, 2 h; *in situ*-(f) Piperazine, CH$_2$Cl$_2$, 25 °C, 12 h (61%); (g) BF$_3$.Et$_2$O, CHCl$_3$, 25 °C, *p*-chloranil, 48 h (14%); (h) 2 N Methanolic KOH, THF/pyridine (10:1), reflux, 24 h (71%); (j) Boc$_2$O, CH$_2$Cl$_2$, 0–25 °C, 24 h (50%); (k) EDCI.HCl, HOBT, Et$_3$N, DMF, 25 °C, 24 h (54%); (m) TFA, CH$_2$Cl$_2$, 25 °C, 1 h (89%). *(Note—all the derivatives of compounds **3**–**4** and compounds **9**–**11**, were present in the two isomers (confirmed by HPLC). However, only one of the possible structures is shown in the above scheme and the other possibility is highlighted by blue and red arrows).*

Nucleophilic Carboxyl-chlorin Intermediate 11 (TPC$_{C1P}$). For structural variation in the study, we also synthesized a functionally different mono-carboxyl chlorin photosensitizer and its key nucleophilic intermediate, as discussed in this section. The starting precursor for the synthesis, methyl-4-formylbenzoate (**5**) was prepared by esterification of 4-formylbenzoic acid using acetyl chloride/MeOH. Porphyrin mono-ester **6** (TPP$_{MC1}$) was then synthesized using methyl-4-formylbenzoate and benzaldehyde (1:3 equiv) and pyrrole (4 equiv) in the presence of a catalytic amount of BF$_3$·OEt$_2$ in CHCl$_3$, by the Lindsey method.[46] Compound **6** was subsequently hydrolyzed by methanolic KOH in THF/pyridine (10:1) to afford compound **7** (TPP$_{C1}$). Column-purified mono-carboxyl-porphyrin **7** was then converted to the corresponding mono-carboxyl-chlorin **8** (TPC$_{C1}$) by the Whitlock diimide reduction, similar to what was discussed in a previous section. However, low solubility of acid **7** in toluene or EtOAc solvents at 25 °C caused some difficulties in the back-oxidation step in this case. At the elevated temperature, the reaction was uncontrollable and led to over-oxidation. This problem was overcome by using a mixture of CH$_2$Cl$_2$/MeOH (3:1), in which the reagents and products were completely soluble at 25 °C. In the end, pure carboxyl-chlorin **8** was obtained and confirmed by ^{1}H NMR, HRMS and UV-vis spectorscopy.

In order to transform carboxyl-chlorin into a strategically important second nucleophilic intermediate, compound **8** was coupled with 1-boc-piperazine **9** using EDCI/HOBt in DMF to obtain the boc-protected amide **10**. Compound **10** was subsequently deprotected using TFA/CH$_2$Cl$_2$ at 25 °C to provide intermediate **11** (TPC$_{C1P}$) (Scheme 1B). Compound **11** was purified and confirmed by NMR, HR-MS and UV-vis spectroscopy before its utilization in the synthesis of TPC$_{C1P}$-chitosan nano-conjugates (**23** and **24**). The ^{1}H NMR analysis showed the two distinct peaks attributed to inner pyrrolic-N*H* of compounds **8** (−1.53, −1.60 ppm) and **11** (−1.40, −1.47 ppm). Also, HPLC analysis confirmed there are two isomers of chlorin compounds **8**

37

(in the ratio 1:0.99), **10** (in the ratio 1:0.94), and **11** (in the ratio 1:0.87), as theoretically presumed (Scheme 1B).

**Amphiphilic Final Nano-conjugates [TPC$_{N1P}$-chitosan (18, 19) and TPC$_{C1P}$-chitosan (23, 24)].**

A well-controlled chemical modification of chitosan has always been challenging due to its low solubility in organic solvent and neutral or alkaline aqueous solutions. In addition, there is always the possibility of cross-reactivity due to its multiple functional groups (*C-2*-NH$_2$, *C-3*-OH and *C-6*-OH). To overcome this problem, we have developed a quantitative method to convert chitosan-mesylate (**12**) into 100% *tert*-butyldimethylsilyl ether (both –OH) protected chitosan **13** (Di-TBDMS-chitosan).[37, 47] This fully *O*-protected precursor **13,** has proved to be very useful as it has a good solubility profile in moderately polar organic solvents and also offers an array of efficient chemoselective *N*-modification.[48-50] Furthermore, its bromoacetyl derivative *N*-bromoacetyl-DiTBDMS-chitosan **14** has been utilized as a key reactive electrophilic intermediate allowing the covalent linkage of hydrophobic as well as hydrophilic moieties with varying DS.[36] Compound **14** can therefore facilitate covalent chlorin modification on chitosan by a nucleophilic substitution reaction with an earlier prepared reactive nucleophilic intermediate **4** (TPC$_{N1P}$) or **11** (TPC$_{C1P}$).

Final TPC-chitosan nano-conjugates (**18, 19** and **23, 24)** were synthesized by reacting the chitosan intermediate **14** and TPC intermediates, either **4** (TPC$_{N1P}$) or **11** (TPC$_{C1P}$), by two slightly different approaches (Scheme 2). For amino-chlorin based nano-conjugates (**18, 19)**, the PS compound **4** (TPC$_{N1P}$) (0.1 equiv) reacted with chitosan compound **14** in the presence of Et$_3$N (0.1 equiv) in CH$_2$Cl$_2$ at 25°C to obtain a 0.1 DS substituted compound **15**. It was then further conjugated with the hydrophilic moieties Me$_3$N or 1-methylpiperazine in CH$_2$Cl$_2$, to afford

corresponding compounds **16** or **17**, respectively. Whereas for carboxyl-chlorin-based nano-conjugates **(23, 24),** PS compound **11** (TPC_{C1P}) (0.1 equiv) was reacted with chitosan compound **14** in the presence of $NaHCO_3$ in *N*-Methyl-2-pyrrolidone (NMP) at 75 °C, to afford compound **20** with 0.1 DS. Compound **20** was further conjugated with the hydrophilic moieties Me_3N or 1-methylpiperazine in CH_2Cl_2, to afford the corresponding compounds **21** or **22**, respectively.

Unexpectedly, the first attempt for final TBDMS deprotection of compounds **16**, **17**, **21**, **22** using tetrabutylammonium fluoride (TBAF) in NMP at 55 °C caused back-oxidation. This was confirmed by ^{1}H NMR as well as UV-vis spectroscopy in which the characteristic band-I peak at 650 nm for chlorin had completely vanished. The mechanism of the reaction that causes back-oxidation is not certain. However it has been reported that TBAF has a role in the oxidation of aromatic aldehydes.[51] Finally, compounds **16**, **17**, **21**, **22** were therefore deprotected by concd HCl in MeOH at 25 °C, followed by aqueous dilution, ion-exchange (with 10% aq NaCl) and dialysis. Finally lyophilization afforded the corresponding final pure chlorin based TPC-chitosan nano-conjugates **(18, 19, 23** and **24).**

Scheme 2. Synthesis of TPC$_{N1P}$-chitosan **(18, 19)** and TPC$_{C1P}$-chitosan **(23, 24)** Nano-conjugates
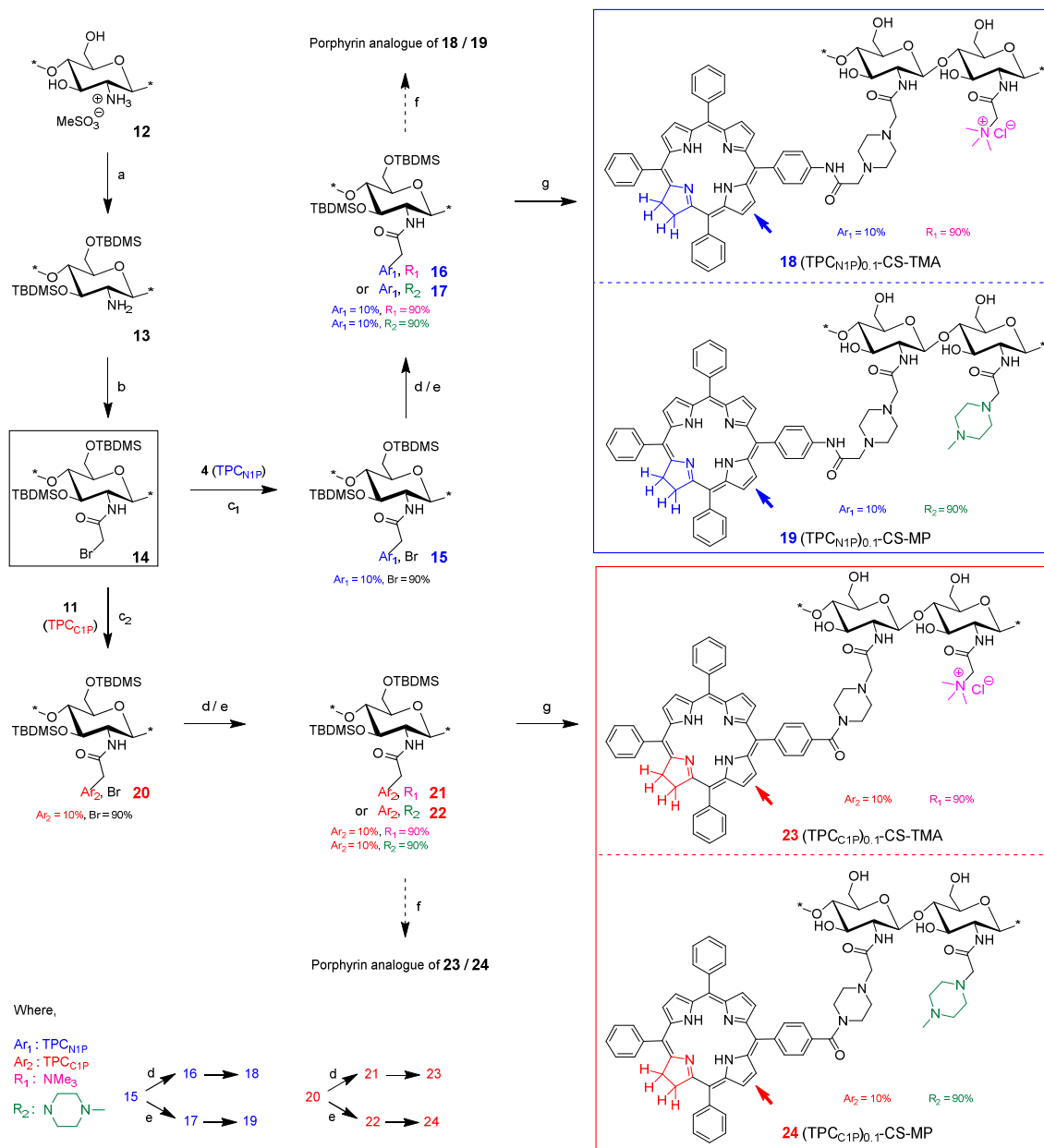
Reagents and conditions: (a) TBDMSCl, imidazole, DMSO, 25 °C, 24 h (96%); (b) Bromoacetyl bromide, Et$_3$N, CH$_2$Cl$_2$, −20 °C, 1 h (92%); (c$_1$) Compound **4** (TPC$_{N1P}$) (0.1 equiv), Et$_3$N, CH$_2$Cl$_2$, 25 °C, 2 h (78%); (c$_2$) Compound **11** (TPC$_{C1P}$) (0.1 equiv), NaHCO$_3$, NMP, 75 °C, 12 h (89%); (d) NMe$_3$ (31−35 wt % in EtOH, 4.2 M), CH$_2$Cl$_2$, 25 °C, 24 h; (e) 1-Methylpiperazine, CH$_2$Cl$_2$, 25 °C, 24 h; (f) TBAF, NMP, 55 °C, 12 h; (g) concd HCl, MeOH, 25 °C.

40

(*Note—all the final nano-conjugates (18, 19, 23 and 24) would most probably exist in two possible chlorin isomers; and blue or red arrows highlight that possibility*).

^{1}H NMR and FT-IR Analysis. All the TPC-chitosan nano-conjugates (**18**, **19**, **23**, and **24**) were completely soluble in pure aqueous conditions and in a mixture of DMSO/H$_2$O (~96:4). However, unlike ^{1}H NMR in DMSO-d_6/D$_2$O (~96:4), peaks belonging to the hydrophobic PS appears to be missing in the aromatic region of the ^{1}H NMR in pure D$_2$O. Similarly, absorbance and fluorescence quenching of these compounds were observed in pure water. This observation was consistent with our earlier study of porphyrin-based TPP-chitosan nano-conjugates. We have proposed the hypothesis that this might be due to π-π stacking and the hydrophobic aggregation of the PS moieties in the core of a nanoparticle-like structure.[36] Therefore, ^{1}H NMR, UV-vis and fluorescence analysis of these nano-conjugates were performed both in pure aqueous conditions and in a mixture of DMSO-d_6/D$_2$O (~96:4). The ^{1}H NMR spectra overlay of the key intermediates and final TPC$_{N1P}$-chitosan (**18, 19**) and TPC$_{C1P}$-chitosan (**23, 24**) nano-conjugates is shown in Figures 3 and 4, respectively. The comparative ^{1}H NMR analysis in corollary to UV-vis analysis, of nano-conjugates (**18, 19, 23** and **24**) with their porphyrin analogues (*data not shown*) confirmed that they are pure chlorins, as no trace amount of porphyrin contamination was observed. This is particularly encouraging as there is always a chance of chlorin being contaminated with a <10% porphyrin side product, as suggested by a few literature examples such as tetra-*meta*-*O*-glycosylated derivative of tetraphenylchlorin identified by ^{1}H NMR.[52]

The FT-IR overlays of key intermediates and final nano-conjugates **18, 19** and **23, 24** are shown in the *Supporting Information*. The small characteristic TPC moiety peaks (794, 703 cm^{-1}) and chitosan (836, 777 cm^{-1}, TBDMS peaks) in the intermediate compounds mark the presence of the covalent attachment of chlorin to chitosan with low DS. The spectra of final nano-conjugates reassure that the characteristic chlorin peaks are intact after the TBDMS deprotection.
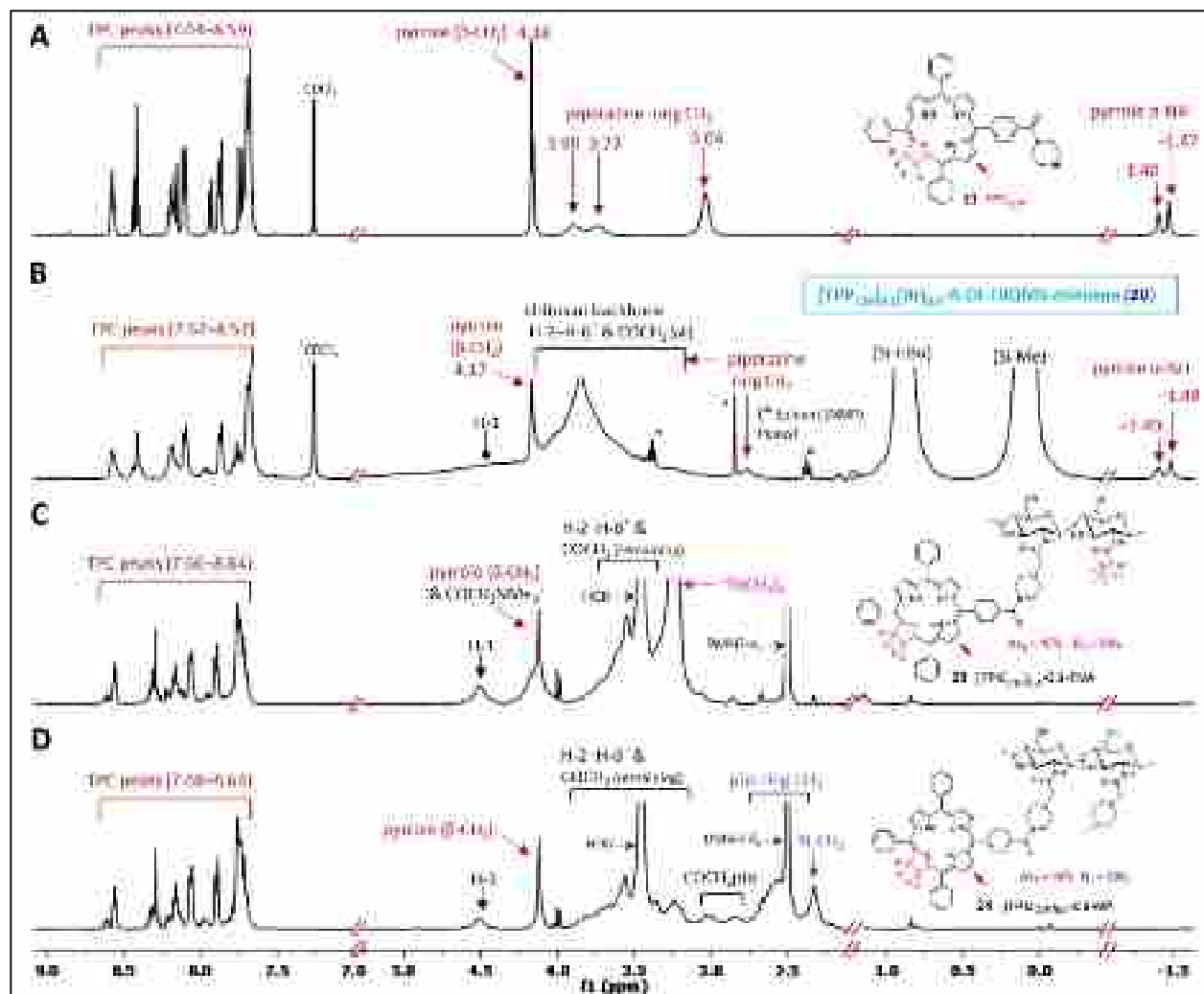
41

Figure 3. ^{1}H NMR spectra overlay of the main intermediate compounds and the final TPC$_{N1P}$-chitosan

conjugates: (A) **4** (TPC$_{N1P}$); (B) **15** [(TPC$_{N1P}$)$_{0.1}$(Br)$_{0.9}$-A-Di-TBDMS-chitosan]; (C) **18** [(TPC$_{N1P}$)$_{0.1}$-CS-

TMA]; (D) **19** [(TPC$_{N1P}$)$_{0.1}$-CS-MP].

Figure 4. ^{1}H NMR spectra overlay of the main intermediate compounds and the final TPC$_{C1P}$-chitosan conjugates: (A) **11** (TPC$_{C1P}$); (B) **20** [(TPC$_{C1P}$)$_{0.1}$(Br)$_{0.9}$-A-DiTBDMS-chitosan]; (C) **23** [(TPC$_{C1P}$)$_{0.1}$-CS-TMA]; (D) **24** [(TPC$_{C1P}$)$_{0.1}$-CS-MP].

GPC Analysis. The molecular weight of the final nano-conjugates is important from a biological point of view. The GPC results suggested that there was a substantial change in the weight-average molecular weight (Mw) and heterogeneity (polydispersity index, PDI) of the material, which took place while converting the parent chitosan material (235 kDa, PDI: 2.77) to its mesylate salt **12** (10.6 kDa, PDI: 1.04). This reduction in Mw must be due to the acidic reaction conditions required for this transformation, which can lead to the degradation of the long polymer chain. The Mw determined for the chitosan mesylate is consistent with the earlier results obtained by MALDI-TOF and the end labelling for chitosan derivatives prepared from chitosan mesylate.[53] The Mw of the final nano-conjugates **18, 19, 23** and **24** were found to be in the range of 4–7 kDa (Table 1), indicating slightly more degradation (as compared to **12**) of the carbohydrate backbone during the multiple-step synthesis process. The PDI is in the range of 1.23–1.28, which shows the relative homogeneity of the polymeric materials. The GPC chromatogram of the representative nano-conjugate **18** is shown in Figure 5A and shows a single peak, which also indicates the purity of the compound.

Physicochemical Properties. The DS for the hydrophobic PSs was determined from the ^{1}H NMR spectra of the intermediate **15** for TPC$_{N1P}$-chitosan (**18** and **19),** and the intermediate **20** for TPC$_{C1P}$-chitosan (**23** and **24**) nano-conjugates. DS was found to be 0.10 for all nano-conjugates (Table 1), which confirms that the covalent linking process of PSs to Di-TBDMS-chitosan was highly efficient, as the amount used in the reaction and the measured linked PSs were in good agreement. The DLS studies revealed that all four TPC-chitosan nano-conjugates formed nanoparticles in an aqueous medium. The average particle size for all nano-conjugates was in the same range, between 140–195 nm. A representative example of particle size distribution of the

44

nanoparticles formed is shown in Figure 5B. Also, the zeta potential of all nano-conjugates shows

that all particles were positively charged in the 80–86 mV range (Table 1). This is consistent with

the good physical stability of the cationic nano-conjugate particles.

Table 1. Physicochemical Properties of the TPC-chitosan Nano-conjugates **(18, 19, 23** and **24)**

Nano-conjugates	No.	Photosensitizer Reacted[a]		DS[b]	Average Particle Size[c] (nm)	ζ potential[c] (mV)	Mw[d] (kDa)	PDI[d]
		TPC_{N1P}	TPC_{C1P}					
$(TPC_{N1P})_{0.1}$-CS-TMA	**18**	0.10	--	0.10	155 ± 96	86 ± 16	5.3	1.28
$(TPC_{N1P})_{0.1}$-CS-MP	**19**	0.10	--	0.10	194 ± 112	83 ± 5	5.8	1.28
$(TPC_{C1P})_{0.1}$-CS-TMA	**23**	--	0.10	0.10	148 ± 59	80 ± 4	6.9	1.23
$(TPC_{C1P})_{0.1}$-CS-MP	**24**	--	0.10	0.10	143 ± 65	83 ± 8	4.5	1.25

[a]*Equivalent per glucosamine monomer unit of chitosan.* [b]*DS determined by* [1]*H NMR.* [c]*DLS and* ζ *potential measurements of all nano-conjugates were done in water.* [d]*Mw and PDI was determined by GPC. For detailed information please see Methods section.*

Absorption and Fluorescence Emission Spectra. Absorption spectra of the TPC-chitosan nano-

conjugates in DMSO show a typical Soret band at around 422 nm and four Q-bands at 521, 549,

598 and 652 nm (Figure 5C). A small bathochromic shift and a marked hyperchromic effect of

the Q-(band-I) at 652 nm could confirm the characteristic peak for typical chlorin derivatives as

compared to porphyrin analogues. The absorption spectra of these nano-conjugates in aqueous

medium shows a broadening and a splitting of the Soret peak into two equal peaks at 408 and 422

nm. Likewise, a broadening of the Q-bands (Figure 5C) at 523, 551, 601 and 654 nm is also

observed. As compared to the absorption in DMSO, absorption at the Soret band was reduced

~1.5 fold in water at equal concentrations, indicating quenching in an aqueous medium.

Similarly, a substantial excited state of the fluorescence quenching of these nano-conjugates was

observed in aqueous solution suggesting an intermolecular association[54] causing aggregation. In comparison, fluorescence quantum efficiency is much higher in DMSO (Figure 5D). The fluorescence emission spectra of TPC-chitosan nano-conjugates show two bands: λ_{max} at 653.5 nm, and a secondary shoulder band λ_{max} at 716.5 nm in DMSO. These peaks show a broadening and a minor blue shift (λ_{max} at 651 and 712 nm) in pure water. The fluorescence maxima in aqueous medium was quenched >12 fold (Figure 7D) compared to that in DMSO, for all TPC-chitosan nano-conjugates.
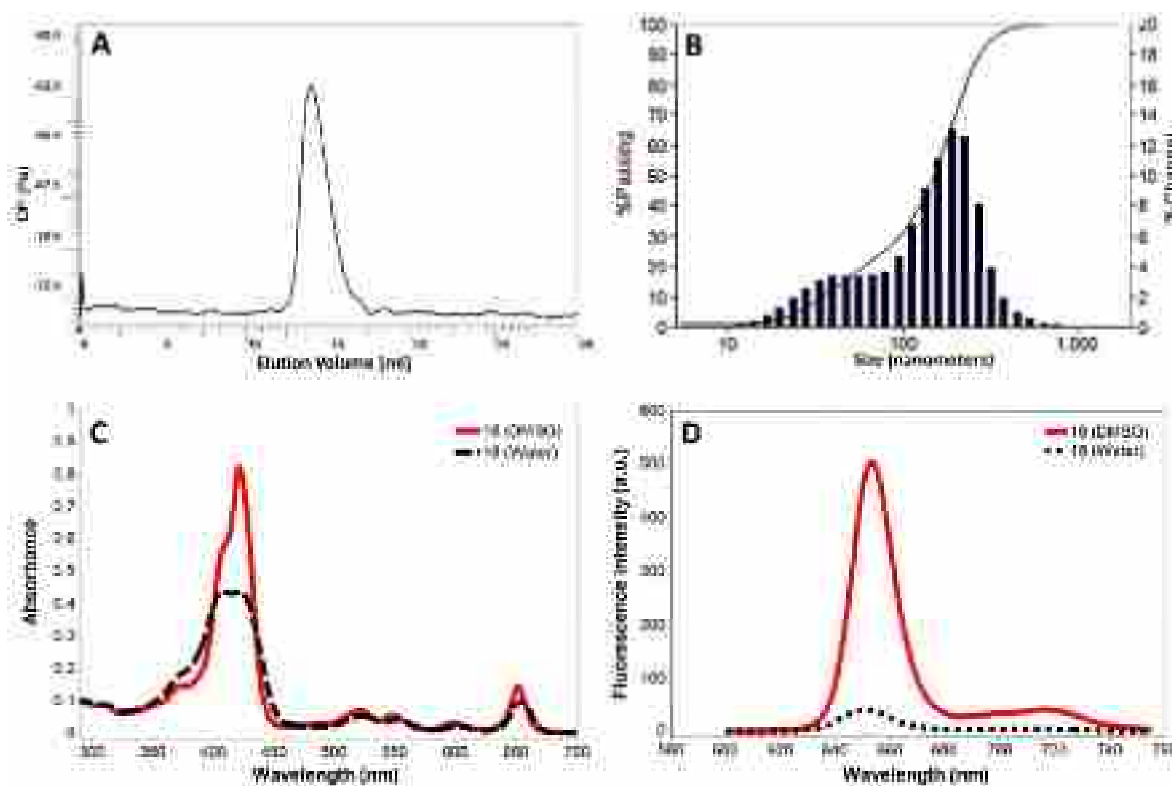

Figure 5. Photophysical results of representative TPC-chitosan nano-conjugate (**18**): (A) GPC chromatogram of viscosity measurement; (B) DLS measurement showing intensity wise particle size distribution; (C) Absorption spectra of **18** in DMSO and water at equal concentrations (0.3 mg/L); (D) Fluorescence emission spectra of **18** in DMSO and water [absorbance adjusted to 0.4 (1 cm path length) for both, and slit width used = 10 for both entrance and exit, λex = 420].

Fluorescence Quantum Yield.

The fluorescence quantum yield (Φ_F) of porphyrin and chlorin derivatives (Table 2) was determined by a steady state comparative method relative to TPP (in toluene, $\Phi_F = 0.11$) as a standard. Among the porphyrin intermediates, the amino-porphyrin derivative (TPP$_{N1P}$) and the carboxyl-porphyrin derivatives—**6** (TPP$_{MC1}$), **7** (TPP$_{C1}$), and TPP$_{C1P}$ have similar Φ_F values to one another. However, Φ_F of the amino-porphyrin **2** (TPP$_{N1}$) was significantly lower (>10 fold) than that of rest of these compounds. Also, unlike for the other compounds, a broadening of the Soret-band (at 419 nm) in the absorption spectrum and a small red-shift in the emission spectrum ($651 \rightarrow 653.5$ nm) was observed. This seems to be due to the electron donor amino group at the *para*-position of the phenyl ring influencing the electron delocalized porphyrin π-conjugated system, and also its possible interactions like H-bonding (N-H$\cdots$O=S)[55] with the solvent DMSO, causing aggregation and consequently fluorescence quenching. A similar finding was reported previously for this compound although in a different solvent (DMF).[56] A similar trend was observed among the chlorin analogues of these compounds, where the carboxyl-chlorin **8** (TPC$_{C1}$), **11** (TPC$_{C1P}$), and the amino-chlorin derivative **4** (TPC$_{N1P}$) had similar Φ_F values, while amino-chlorin **3** (TPC$_{N1}$) had a significantly lower (>5 fold) Φ_F value. Between the porphyrin and chlorin counterparts of the aryl-amine, Φ_F of **3** (TPC$_{N1}$) was approximately >5 fold higher than **2** (TPP$_{N1}$). The increase in the fluorescence intensity of chlorin PSs can possibly be explained as being due to the distorted planarity caused by the reduced double bond of one of the pyrrole rings of the chlorin system compared to the planar π-stabilized porphyrinic system. A substantial enhancement in Φ_F was detected after further derivatization of the amino-porphyrin/chlorin **2/3**

47

(TPP$_{N1}$/TPC$_{N1}$). This is probably because when TPP$_{N1}$/TPC$_{N1}$ (**2**/**3**) is chemically transformed into TPP$_{N1P}$/TPC$_{N1P}$ **4**, the electron flow of the amino group drives to the opposite direction of the aromatic system through the amide linker (in TPP$_{N1P}$/TPC$_{N1P}$), and also a possible distortion in planarity may contribute to a rise in the Φ_F. Other chlorin compounds (**8, 11**) showed a ~3 fold enhancement in Φ_F compared to their porphyrin analogues.

The conjugation of these PSs to chitosan or the structure of the spacer group (**18, 19, 23 and 24**) did not affect their Φ_F in DMSO. These chlorin-chitosan nano-conjugates **18** and **19** demonstrated a ~3-fold enhancement in their Φ_F compared to their counterpart porphyrin-chitosan nano-conjugates (Table 2). The Φ_F values of all the final TPC-chitosan nano-conjugates closely match (Table 2) that of fimaporfin (TPCS$_{2a}$), which could suggest their efficiency as a fluorophore for PCI. The Φ_F of the nano-conjugates (**18, 19, 23** and **24**) in water demonstrated a high degree of excited state quenching (>12 fold lower Φ_F) compared to when in DMSO. Among the nano-conjugates, **19** showed the lowest, whereas **18** showed a higher Φ_F in an aqueous medium. It is, however, difficult to predict what is causing this difference as a similar trend was not seen in the case of **23** and **24**. The Φ_F values are dependent on many factors such as standards, solvents, *etc.* Therefore, literature examples of the same compound with identical measurement conditions are difficult to find for direct comparison. We observed that our calculated values are in the same range as those of a few reported examples for similar compounds with TPP as a standard,[57-59] although the solvents were different. Also, discrepancies in the values of Φ_F could inevitably be observed when compared to examples where different standards such as quinine sulfate,[60] Rhodamine B,[52] and hematoporphyrin,[61] have been used. We found that TPP is better suited as a standard for our measurements as it completely overlaps with the absorbance and fluorescence. Please see the *Supporting Information* for a detailed illustration of this.

48

Table 2. Absorption and Fluorescence Properties of the Key Porphyrin and Chlorin Intermediates and Final Chitosan Nano-conjugates

| Broad Classification	Compd	No.	λ_{max} (nm)	λ_{ex} (nm)	λ_{em} (nm)	$\Phi_F{}^a$
Mono-amino derivatives (in DMSO)						
Porphyrin	TPP_{N1}	**2**	419	419	653.5	0.015
Chlorin	TPC_{N1}	**3**	421	421	654.5	0.081 ± 0.002
Porphyrin	TPP_{N1P}	$-^b$	419	419	651	0.164 ± 0.005
Chlorin	TPC_{N1P}	**4**	422	422	654	0.456 ± 0.013
Porphyrin-chitosan	$(TPP_{N1P})_{0.1}$-CS-TMA	$-^b$	420	420	651	0.144 ± 0.009
Chlorin-chitosan	$(TPC_{N1P})_{0.1}$-CS-TMA	**18**	421	421	654	0.437 ± 0.013
Porphyrin-chitosan	$(TPP_{N1P})_{0.1}$-CS-MP	$-^b$	420	420	651	0.143 ± 0.005
Chlorin-chitosan	$(TPC_{N1P})_{0.1}$-CS-MP	**19**	421	421	654	0.454 ± 0.013
Mono-carboxyl derivatives (in DMSO)						
Porphyrin	TPP_{MC1}	**6**	419	419	649	0.155 ± 0.005
Porphyrin	TPP_{C1}	**7**	419	419	649.5	0.158 ± 0.005
Chlorin	TPC_{C1}	**8**	421	422	654	0.457 ± 0.013
Porphyrin	TPP_{C1P}	$-^b$	419	419	648.5	0.149 ± 0.004
Chlorin	TPC_{C1P}	**11**	420	421	654	0.488 ± 0.014
Chlorin-chitosan	$(TPC_{C1P})_{0.1}$-CS-TMA	**23**	421	421	654	0.452 ± 0.013
Chlorin-chitosan	$(TPC_{C1P})_{0.1}$-CS-MP	**24**	420	421	654	0.436 ± 0.013
Chlorin	$TPCS_{2a}$ (fimaporfin)		421	421	656	0.478 ± 0.030
Φ_F of Chlorin-chitosan compounds (in H_2O)						
Chlorin-chitosan	$(TPC_{N1P})_{0.1}$-CS-TMA	**18**	427.5	420	651	0.035 ± 0.001
Chlorin-chitosan	$(TPC_{N1P})_{0.1}$-CS-MP	**19**	428	420	651	0.013
Chlorin-chitosan	$(TPC_{C1P})_{0.1}$-CS-TMA	**23**	425	420	650	0.026 ± 0.001
Chlorin-chitosan	$(TPC_{C1P})_{0.1}$-CS-MP	**24**	423	420	654	0.023 ± 0.001

[a]Φ_F of all compds were determined relative to reference standard TPP ($\Phi_F = 0.11$, toluene). For detailed information please see the Supporting Information. [b]These compounds are synthesized for comparison purposes only and are not shown in the schemes of the current manuscript. λ_{max} is the absorbance maxima of UV-vis

spectra, λ_{ex} is the excitation wavelength used for the fluorescence emission spectra; λ_{em} is the emission maxima (band-I).

Biological Studies

In Vitro Study

Cellular Uptake and Localization. The cellular uptake and subcellular localization of the nano-conjugates were studied by fluorescence microscopy using ovalbumin as a marker molecule for uptake into endocytic vesicles. It can be seen that after a relevant time for PCI treatment (24 and 48 h), nano-conjugates **19** and **23** had been efficiently taken up by the cells and co-localized almost completely with the endocytosis marker ovalbumin (Figure 6). This shows that after cellular uptake, these compounds very specifically localize to the vesicles that are relevant for PCI-mediated delivery of a macromolecular drug to the cytosol. Similar results were found for nano-conjugates **18** and **24** (*data not shown*). Strong fluorescence of the compounds indicated that the conjugates contained in the self-aggregated nano-conjugate particles unfold and become photochemically active to allow the lipophilic photosentizer moieties to be inserted into the endosomal membrane. Thus, the fluorescence is no longer quenched.[36]
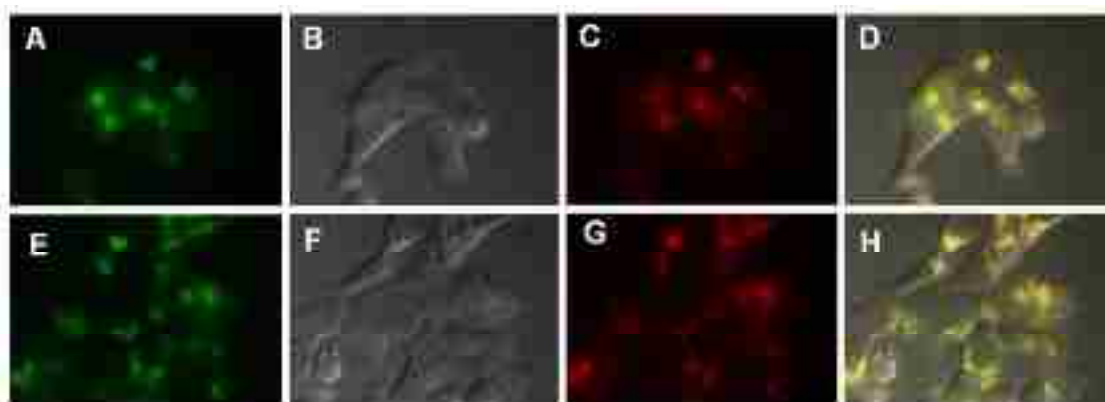
Figure 6. Subcellular localization of nano-conjugates **19** and **23**. HCT 116 cells were incubated with the nano-conjugates **19** and **23** in concentrations corresponding to 1 µg/mL of photosensitizer and 25 µg/mL Alexa-488 labelled ovalbumin as a marker for endocytic vesicles. Fluorescence microscopy was performed after 24 h ((**19**) (A-D)) or 48 h (**23**) (E-H) as described under *Biological Methods Section*. Panels A and E: Alexa-488 ovalbumin fluorescence; B and F: phase contrast; C and G: TPC fluorescence; D and H: merge of Alexa-488 and TPC fluorescence, yellow color denotes co-localization of the markers.

Use of the Nano-conjugates for PCI-mediated Transfection. The biological effects of the TPC$_{N1P}$-chitosan **(18, 19)** and TPC$_{C1P}$-chitosan **(23, 24)** were tested in experiments where the nano-conjugates were used as photosensitizing agents in photochemical internalization to enhance gene delivery. The experimental details are described in the *Biological Materials and Methods section*. As can be seen in Figure 7 (A, B) the TPC$_{N1P}$-chitosan nano-conjugates **18** and **19** were excellent photosensitizers for PCI, in that a substantial enhancement of transfection could already be observed at low light doses. Similar results could be seen in case of TPC$_{C1P}$-chitosan nano-conjugates **23** and **24** [Figures 7 (C, D)] showing that these nano-conjugates are also effective in inducing a PCI effect.
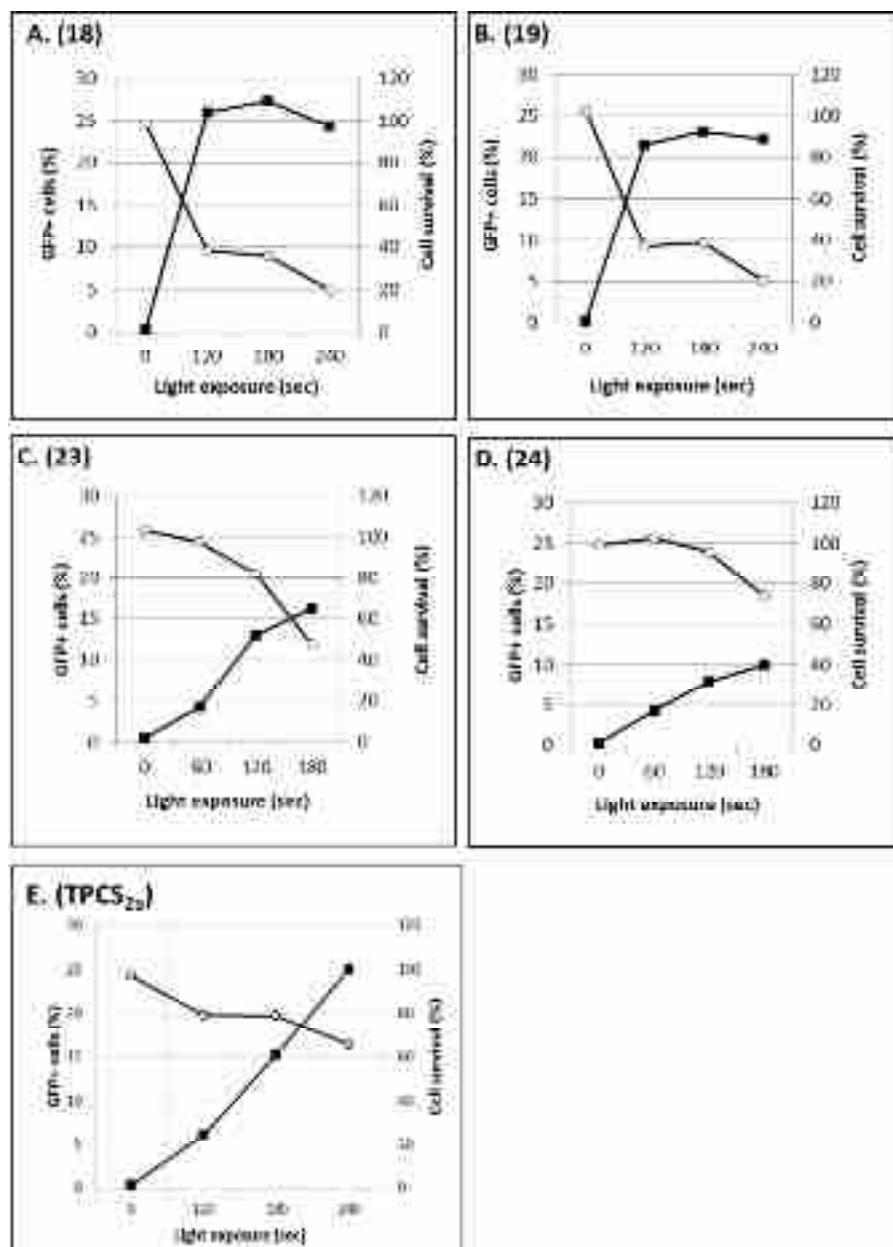
Figure 7. Transfection of the TPC-chitosan nano-conjugates with the plasmid encoding enhanced green fluorescent protein (pEGFP-N1) in HCT116/LUC cells. Transfection was measured 48 h after illumination by flow cytometry. Cell survival was measured by the MTT assay: (A) Nano-conjugate **18**. 0.05 μg/mL TPC; (B) Nano-conjugate **19**. 0.05 μg/mL TPC; (C) Nano-conjugate **23**. 0.05 μg/mL TPC; (D) Nano-conjugate **24**. 0.05 μg/mL TPC.

52

In Vivo Study

The TPC-chitosan nano-conjugates have also been explored in preliminary *in vivo* experiments, investigating whether the nano-conjugates are active in PDT- and PCI-based therapeutic approaches. Figure 8 shows pictures of illuminated tumor-bearing mice treated with the nano-conjugates **24** and **19** either alone or together with the cytotoxic anti-cancer agent bleomycin (for details see *Biological Methods section*).
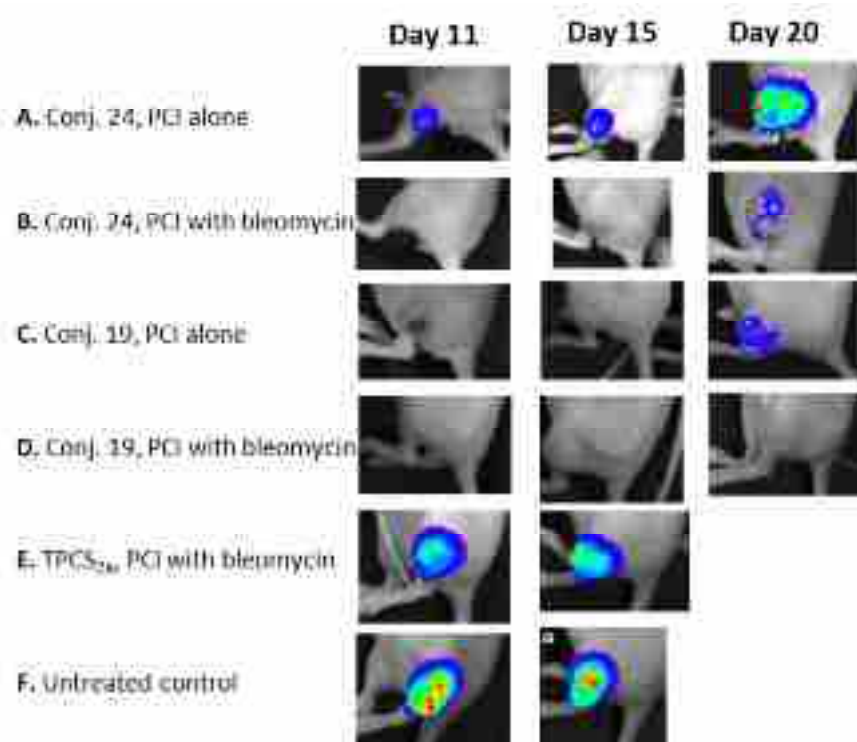
Figure 8. *In vivo* bioluminescence imaging after PCI treatment of HCT116/Luc tumor-bearing animals with TPC-chitosan nano-conjugates (24 and 19) and bleomycin. The treatment for each animal and the time point for imaging (days after photosensitizer injection) are indicated in the figure.

The cancer cells used were permanently transfected to express luciferase so that the extent of the tumors could be monitored by bioluminescence imaging after the injection of luciferin. As shown

in Figure 8, the untreated control (animal **F**) exhibited strong tumor bioluminescence 11 and 15 days after injection of the photosensitizer (7 and 11 days after illumination), indicating the presence of large amounts of living cancer cells in the tumor. In these animals, the tumors had grown so large that the animals had to be sacrificed for ethical reasons after day 15. In contrast, for animals treated with the chitosan nano-conjugates, there was only weak bioluminescence in some of the animals (A, C and D) at day 11, showing that both the photochemical treatment (analogous to a PDT treatment) and the PCI of bleomycin combination treatment had strongly reduced the amount of cancer cells in the tumor. It can be observed that the fluorescence increased through day 15 to day 20 in the animals treated with photosensitizer and light only (animals **A** and **C**), showing that the photochemical treatment alone was not sufficient to kill all the tumor cells. In contrast, the animals treated with PCI + bleomycin (animals **B** and **D**) showed essentially no bioluminescence, even at day 20, showing that this combination was significantly more effective than PCI alone. This indicates that the TPC-chitosan nano-conjugates induced a strong photochemical internalization effect.

CONCLUSION

We have optimized a method for the preparation of two different highly lipophilic mono-functional *meso*-tetraphenylchlorin based PSs, namely TPC_{N1} and TPC_{C1}. These chlorin PSs obtained as pure compounds, free of TPP contamination, and were utilized for the efficient synthesis of four distinct, amphiphilic chitosan-based nano-conjugates. Nucleophilic derivatives of these PSs (TPC_{N1P} and TPC_{C1P}) and an electrophilic chitosan intermediate (*N*-bromoacetyl-Di-TBDMS-chitosan) were first conjugated with the controlled 0.1 DS of PSs. Then, the hydrophilic

54

moieties trimethylamine or 1-methylpiperazine were incorporated and finally a TBDMS was deprotected. Covalent attachment and controlled substitution of the PSs and hydrophilic moieties were confirmed by ^{1}H NMR, FT-IR and GPC analysis. All four nano-conjugates are polar and are completely soluble in water, forming nanoparticles under aqueous conditions. The NMR, UV-vis and fluorescence analyses of these nano-conjugates were consistent with the self-association of hydrophobic PS moieties as per our earlier hypotheses stated in the case of TPP based nano-conjugates.[36] In an aqueous medium, the nano-conjugates assemble into nanoparticle-like structures with cationic polymer backbones forming the outer shell around aggregated π-π stacked TPC moieties. In comparison, the cationic polymer backbones are freely movable in DMSO and show a dramatic rise in fluorescence due to dissociation of PS moieties; a similar unfolding appears to take place when the photosensitizers are in contact with the cell or endocytic vesicle membranes, as indicated by a strong fluorescence in cellular systems. Being a highly pure chlorins, all the nano-conjugates can absorb red light that penetrates deeply into tissues and the quantum yield of the TPC-chitosan nano-conjugates are three-fold higher than that of their porphyrin analogues.

In vitro experiments in a cancer cell line show that all four of these TPC-chitosan based nano-conjugates locate in endocytic vesicles and give excellent light induced enhancement of plasmid transfection even at low light doses. In addition, a preliminary *in vivo* study indicated that the TPC-chitosan nano-conjugates induced a strong photochemical effect alone and a very good PCI effect when used with the cytotoxic anti-cancer agent bleomycin.

ASSOCIATED CONTENT

Supporting Information. The Supporting Information containing the copies of ^{1}H, ^{13}C NMR, HRMS, HPLC, GPC, DLS and Fluorescence emission spectra of the key compounds.is available free of charge via the internet at http://pubs.acs.org.

AUTHOR INFORMATION

Corresponding Author

*Már Másson. Phone: +354-8228301. Fax: +354-5254071. E-mail: mmasson@hi.is
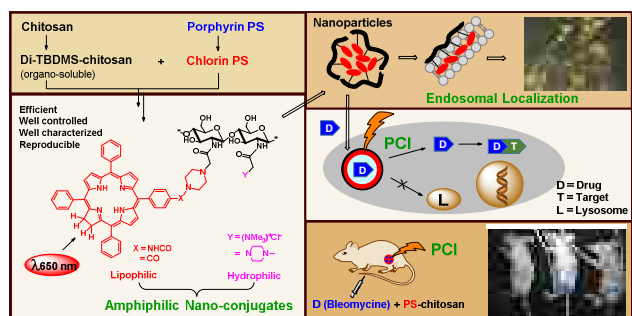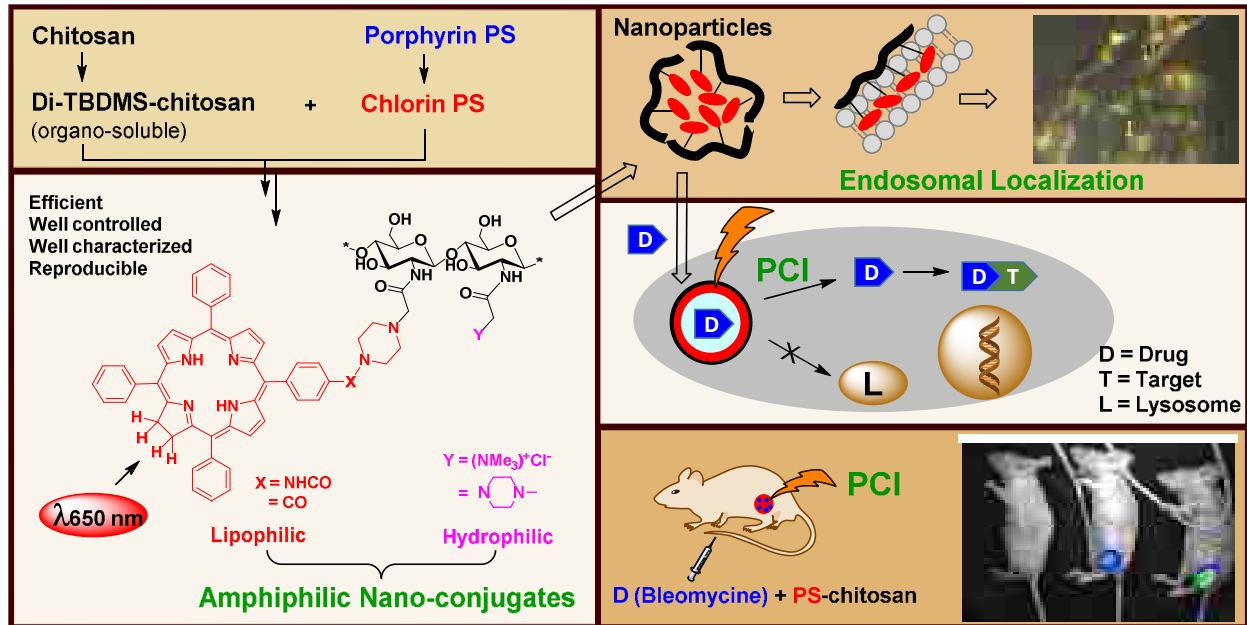
Notes

ACKNOWLEDGMENTS

REFERENCES

(1)   Bayona, A. M. D.; Moore, C. M.; Loizidou, M.; MacRobert, A. J.; Woodhams, J. H., *Int. J. Cancer* **2016,** 138 (5), 1049.

(2)   Berg, K.; Selbo, P. K.; Prasmickaite, L.; Tjelle, T. E.; Sandvig, K.; Moan, D.; Gaudernack, G.; Fodstad, O.; Kjolsrud, S.; Anholt, H.; Rodal, G. H.; Rodal, S. K.; Hogset, A., *Cancer Res.* **1999,** 59 (6), 1180.

(3)   Berg, K.; Folini, M.; Prasmickaite, L.; Selbo, P. K.; Bonsted, A.; Engesaeter, B. O.; Zaffaroni, N.; Weyergang, A.; Dietze, A.; Maelandsmo, G. M.; Wagner, E.; Norum, O. J.; Hogset, A., *Curr Pharm Biotechnol.* **2007,** 8 (6), 362.

(4)   Selbo, P. K.; Weyergang, A.; Hogset, A.; Norum, O. J.; Berstad, M. B.; Vikdal, M.; Berg, K., *J. Contr. Rel.* **2010,** 148 (1), 2.

(5)   Olsen, C. E.; Berg, K.; Selbo, P. K.; Weyergang, A., *Free Radic. Biol. Med.* **2013,** 65 1300.

(6)   Bostad, M.; Olsen, C. E.; Peng, Q.; Berg, K.; Hogset, A.; Selbo, P. K., *J. Contr. Rel.* **2015,** 206 37.

(7)   Engesaeter, B. O.; Tveito, S.; Bonsted, A.; Engebraaten, O.; Berg, K.; Maelandsmo, G. M., *J. Gene. Med.* **2006,** 8 (6), 707.

(8)   Berg, K.; Berstad, M.; Prasmickaite, L.; Weyergang, A.; Selbo, P. K.; Hedfors, I.; Hogset, A. In *Nucleic Acid Transfection*, Bielke, W.; Erbacher, C., Eds. 2010; Vol. 296, pp 251.

(9)   Baglo, Y.; Hagen, L.; Hogset, A.; Drablos, F.; Otterlei, M.; Gederaas, O. A., *Biomed Research International* **2014,** Article ID 921296 10 pages.

(10)   Berg, K.; Nordstrand, S.; Selbo, P. K.; Diem, T. T. T.; Angell-Petersen, E.; Hogset, A., *Photochem. Photobiol. Sci.* **2011,** 10 (10), 1637.

(11)   Park, H.; Park, W.; Na, K., *Biomaterials* **2014,** 35 (27), 7963.

(12)   Dietze, A.; Peng, Q.; Selbo, P. K.; Kaalhus, O.; Muller, C.; Bown, S.; Berg, K., *Br. J. Cancer,* **2005,** 92 (11), 2004.

(13)   Hogset, A.; Engesaeter, B. O.; Prasmickaite, L.; Berg, K.; Fodstad, O.; Maelandsmo, G. M., *Cancer Gene Ther.* **2002,** 9 (4), 365.

(14)   Hogset, A.; Prasmickaite, L.; Selbo, P. K.; Hellum, M.; Engesaeter, B. O.; Bonsted, A.; Berg, K., *Adv. Drug Deliv. Rev.* **2004,** 56 (1), 95.

(15)   Selbo, P. K.; Hogset, A.; Prasmickaite, L.; Berg, K., *Tumour Biol.* **2002,** 23 (2), 103.

(16)   Sternberg, E. D.; Dolphin, D.; Bruckner, C., *Tetrahedron* **1998,** 54 (17), 4151.

(17)   Sultan, A. A.; Jerjes, W.; Berg, K.; Hogset, A.; Mosse, C. A.; Hamoudi, R.; Hamdoon, Z.; Simeon, C.; Carnell, D.; Forster, M.; Hopper, C., *Lancet Oncol.* **2016,** 17 (9), 1217.

(18)   PCIBiotech Amphinex based PCI. http://pcibiotech.no/about-pci-biotech/ (15.07.2015),

(19)   ClinicalTrials.Gov   Amphinex   based   PCI   studies.   . https://clinicaltrials.gov/ct2/results?term=PCI+BIOTECH

(20)   Carcenac, M.; Larroque, C.; Langlois, R.; van Lier, J. E.; Artus, J. C.; Pelegrin, A., *Photochem. Photobiol.* **1999,** 70 (6), 930.

(21)   van Dongen, G.; Visser, G. W.; Vrouenraets, M. B., *Adv. Drug Deliv. Rev.* **2004,** 56 (1), 31.

(22)   Vrouenraets, M. B.; Visser, G. W. M.; Stewart, F. A.; Stigter, M.; Oppelaar, H.; Postmus, P. E.; Snow, G. B.; van Dongen, G., *Cancer Res.* **1999,** 59 (7), 1505.

(23)   Cavanaugh, P. G., *Breast Cancer Res.Trea.* **2002,** 72 (2), 117.

(24)   Hamblin, M. R.; Newman, E. L., *J. Photochem. Photobiol. B* **1994,** 26 (2), 147.
(25)   Hamblin, M. R.; Miller, J. L.; Rizvi, I.; Ortel, B.; Maytin, E. V.; Hasan, T., *Cancer Res.* **2001,** 61 (19), 7155.
(26)   Soukos, N. S.; Hamblin, M. R.; Hasan, T., *Photochem. Photobiol.* **1997,** 65 (4), 723.
(27)   Zhou, Q.; Xu, L.; Liu, F.; Zhang, W. A., *Polymer* **2016,** 97 323.
(28)   Chang, K. W.; Tang, Y.; Fang, X. F.; Yin, S. Y.; Xu, H.; Wu, C. F., *Biomacromolecules* **2016,** 17 (6), 2128.
(29)   Chen, H. B.; Xiao, L.; Anraku, Y.; Mi, P.; Liu, X. Y.; Cabral, H.; Inoue, A.; Nomoto, T.; Kishimura, A.; Nishiyama, N.; Kataoka, K., *J. Am. Chem. Soc.* **2014,** 136 (1), 157.
(30)   Xu, J. S.; Zeng, F.; Wu, H.; Hu, C. P.; Wu, S. Z., *Biomacromolecules* **2014,** 15 (11), 4249.
(31)   Chen, X.; Hui, L.; Foster, D. A.; Drain, C. M., *Biochemistry* **2004,** 43 (34), 10918.
(32)   Di Stasio, B.; Frochot, C.; Dumas, D.; Even, P.; Zwier, J.; Muller, A.; Didelon, J.; Guillemin, F.; Viriot, M. L.; Barberi-Heyob, M., *Eur. J. Med. Chem.* **2005,** 40 (11), 1111.
(33)   Zheng, G.; Graham, A.; Shibata, M.; Missert, J. R.; Oseroff, A. R.; Dougherty, T. J.; Pandey, R. K., *J. Org. Chem.* **2001,** 66 (26), 8709.
(34)   Han, J.; Park, W.; Park, S. J.; Na, K., *ACS Appl. Mater. Interfaces* **2016,** 8 (12), 7739.
(35)   Mazzaglia, A.; Bondi, M. L.; Scala, A.; Zito, F.; Barbieri, G.; Crea, F.; Vianelli, G.; Mineo, P.; Fiore, T.; Pellerito, C.; Pellerito, L.; Costa, M. A., *Biomacromolecules* **2013,** 14 (11), 3820.
(36)   Gaware, V. S.; Håkerud, M.; Leósson, K.; Jónsdóttir, S.; Høgset, A.; Berg, K.; Másson, M., *J. Med. Chem.* **2013,** 56 (3), 807.
(37)   Song, W.; Gaware, V. S.; Rúnarsson, Ö. V.; Másson, M.; Mano, J. F., *Carbohyd. Polym.* **2010,** 81 140.
(38)   Seybold, P. G.; Gouoterman, M., *J. Mol. Spectrosc.* **1969,** 31 1.
(39)   Demas, J. N.; Crosby, G. A., *J. Phys. Chem.* **1971,** 75 (8), 991.
(40)   Adler, A. D.; Longo, F. R.; Finarelli, J. D.; Goldmacher, J.; Assour, J.; Korsakoff, L., *J. Org. Chem.* **1967,** 32 (2), 476.
(41)   Luguya, R.; Jaquinod, L.; Fronczek, F. R.; Vicente, A. G. H.; Smith, K. M., *Tetrahedron* **2004,** 60 (12), 2757.
(42)   Whitlock, H. W.; Hanauer, R.; Oester, M. Y.; Bower, B. K., *J. Am. Chem. Soc.* **1969,** 91 (26), 7485.
(43)   Nascimento, B. F. O.; Gonsalves, A.; Pineiro, M., *Inorg. Chem. Commun.* **2010,** 13 (3), 395.
(44)   Serra, A. C.; Gonsalves, A., *Tetrahedron Lett.* **2010,** 51 (32), 4192.
(45)   Bonnett, R.; White, R. D.; Winfield, U. J.; Berenbaum, M. C., *Biochem. J* **1989,** 261 (1), 277.
(46)   Lindsey, J. S.; Hsu, H. C.; Schreiman, I. C., *Tetrahedron Lett.* **1986,** 27 (41), 4969.
(47)   Rúnarsson, Ö. V.; Malainer, C.; Holappa, J.; Sigurdsson, S. T.; Másson, M., *Carbohyd. Res.* **2008,** 343 2576.
(48)   Gaware, V. S.; Benediktsdóttir, B. E.; Másson, M. In *Chitin and Chitosan Derivatives: Advances in Drug Discovery and Developments*, Kim, S.-K., Ed. CRC-Taylor & Francis: New York, 2013; pp 69.
(49)   Sahariah, P.; Snorradottir, B. S.; Hjalmarsdottir, M. A.; Sigurjonsson, O. E.; Masson, M., *J. Mater. Chem. B* **2016,** 4 (27), 4762.
(50)   Sahariah, P.; Sorensen, K. K.; Hjalmarsdottir, M. A.; Sigurjonsson, O. E.; Jensen, K. J.; Masson, M.; Thygesen, M. B., *Chem. Commun.* **2015,** 51 (58), 11611.
(51)   Chung, K. H.; Moon, B. C.; Lim, C. H.; Kim, J. P.; Lee, J. H.; Chi, D. Y., *Bull. Korean Chem. Soc.* **2006,** 27 (8), 1203.
(52)   Laville, I.; Figueiredo, T.; Loock, B.; Pigaglio, S.; Maillard, P.; Grierson, D. S.; Carrez, D.; Croisy, A.; Blais, J., *Bioorg. Med. Chem.* **2003,** 11 (8), 1643.
(53)   Benediktsdottir, B. E.; Sorensen, K. K.; Thygesen, M. B.; Jensen, K. J.; Gudjonsson, T.; Baldursson, O.; Masson, M., *Carbohyd. Polym.* **2012,** 90 (3), 1273.
(54)   Oulmi, D.; Maillard, P.; Vever-Bizet, C.; Momenteau, M.; Brault, D., *Photochem. Photobiol.* **1998,** 67 (5), 511.
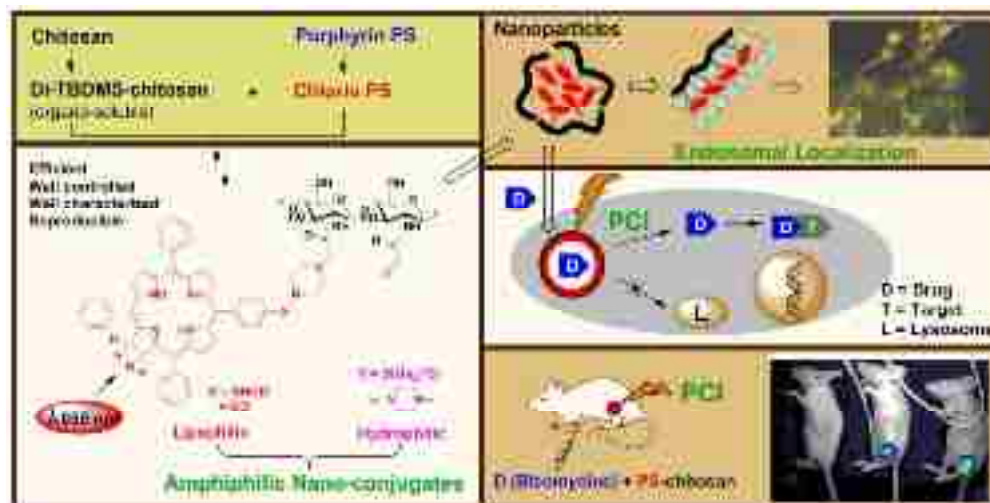(55)   Krystkowiak, E.; Dobek, K.; Maciejewski, A., *J. Photochem. Photobiol. A* **2006,** 184 (3), 250.

58

(56)   Bhaumik, J.; Weissleder, R.; McCarthy, J. R., *J. Org. Chem.* **2009,** 74 (16), 5894.

(57)   Fagadar-Cosma, E.; Cseh, L.; Badea, V.; Fagadar-Cosma, G.; Vlascici, D., *Comb. Chem. High Throughput Screen.* **2007,** 10 (6), 466.

(58)   Milanesio, M. E.; Alvarez, M. G.; Yslas, E. I.; Borsarelli, C. D.; Silber, J. J.; Rivarola, V.; Durantini, E. N., *Photochem. Photobiol.* **2001,** 74 (1), 14.

(59)   Silva, J. N.; Silva, A. M. G.; Tome, J. P.; Ribeiro, A. O.; Domingues, M. R. M.; Cavaleiro, J. A. S.; Silva, A. M. S.; Graca, M.; Neves, M.; Tome, A. C.; Serra, O. A.; Bosca, F.; Filipe, P.; Santuse, R.; Morliere, P., *Photochem. Photobiol. Sci.* **2008,** 7 (7), 834.

(60)   Lilletvedt, M.; Tonnesen, H. H.; Hogset, A.; Nardo, L.; Kristensen, S., *Pharmazie* **2010,** 65 (8), 588.

(61)   Bonnett, R.; Charlesworth, P.; Djelal, B. D.; Foley, S.; McGarvey, D. J.; Truscott, T. G., *J. Chem. Soc., Perkin Trans. 2* **1999,** (2), 325.

Table of Contents Graphic (TOC)

TOC graphic

166x84mm (300 x 300 DPI)